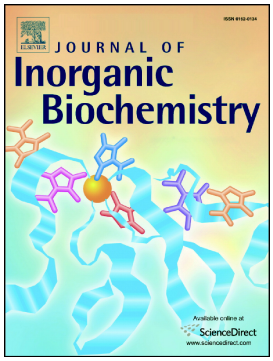

Mononuclear gold(III) complexes with phenanthroline ligands as efficient inhibitors of angiogenesis: A comparative study with auranofin and sunitinib

Aleksandar Pavic, Biljana Đ. Glišić, Sandra Vojnovic, Beata Warżajtis, Nada D. Savić, Marija Antić, Slavko Radenković, Goran V. Janjić, Jasmina Nikodinovic-Runic, Urszula Rychlewska, Miloš I. Djuran

PII: S0162-0134(17)30301-X
DOI: doi: 10.1016/j.jinorgbio.2017.06.009
Reference: JIB 10239

To appear in: *Journal of Inorganic Biochemistry*

Received date: 26 April 2017
Revised date: 20 June 2017
Accepted date: 22 June 2017

Please cite this article as: Aleksandar Pavic, Biljana Đ. Glišić, Sandra Vojnovic, Beata Warżajtis, Nada D. Savić, Marija Antić, Slavko Radenković, Goran V. Janjić, Jasmina Nikodinovic-Runic, Urszula Rychlewska, Miloš I. Djuran , Mononuclear gold(III) complexes with phenanthroline ligands as efficient inhibitors of angiogenesis: A comparative study with auranofin and sunitinib, *Journal of Inorganic Biochemistry* (2017), doi: 10.1016/j.jinorgbio.2017.06.009

Ms. No. JINORGBIO_2017_213 (revised version)

Mononuclear gold(III) complexes with phenanthroline ligands as efficient inhibitors of angiogenesis: a comparative study with auranofin and sunitinib

Aleksandar Pavic[a,*], Biljana Đ. Glišić[b,*], Sandra Vojnovic[a], Beata Warżajtis[c], Nada D. Savić[b], Marija Antić[b], Slavko Radenković[b], Goran V. Janjić[d], Jasmina Nikodinovic-Runic[a], Urszula Rychlewska[c], Miloš I. Djuran[b,e]

[a]*Institute of Molecular Genetics and Genetic Engineering, University of Belgrade, Vojvode Stepe 444a, 11000 Belgrade, Serbia*

[b]*University of Kragujevac, Faculty of Science, Department of Chemistry, R. Domanovića 12, PO Box 60, 34000 Kragujevac, Serbia*

[c]*Faculty of Chemistry, Adam Mickiewicz University, Umultowska 89B, 61-614 Poznań, Poland*

[d]*Institute of Chemistry, Metallurgy and Technology, University of Belgrade, Njegoševa 12, 11000 Belgrade, Serbia*

[e]*Serbian Academy of Sciences and Arts, Knez Mihailova 35, 11000 Belgrade, Serbia*

[*]Corresponding authors: Tel.: +381 11 397 6034; fax: +381 11 397 5808 (A. Pavic); Tel.: +381 34 300 251; fax: +381 34 335 040 (B. Đ. Glišić).

E-mail addresses: sasapavic@imgge.bg.ac.rs (A. Pavic); bglisic@kg.ac.rs (B. Đ. Glišić).

Abstract

Gold(III) complexes with 1,7- and 4,7-phenanthroline ligands, [$AuCl_3$(1,7-phen-κ*N*7)] (**1**) and [$AuCl_3$(4,7-phen-κ*N*4)] (**2**) were synthesized and structurally characterized by spectroscopic (NMR, IR and UV-vis) and single-crystal X-ray diffraction techniques. In these complexes, 1,7- and 4,7-phenanthrolines are monodentatedly coordinated to the Au(III) ion through the N7 and N4 nitrogen atoms, respectively. In comparison to the clinically relevant anti-angiogenic compounds auranofin and sunitinib, gold(III)-phenanthroline complexes showed from 1.5- to 20-fold higher anti-angiogenic potential, and 13- and 118-fold lower toxicity. Among the tested compounds, complex **1** was the most potent and may be an excellent anti-angiogenic drug candidate, since it showed strong anti-angiogenic activity in zebrafish embryos achieving IC_{50} value (concentration resulting in an anti-angiogenic phenotype at 50% of embryos) of 2.89 μM, while had low toxicity with LC_{50} value (the concentration inducing the lethal effect of 50% embryos) of 128 μM. Molecular docking study revealed that both complexes and ligands could suppress angiogenesis targeting the multiple major regulators of angiogenesis, such as the vascular endothelial growth factor receptor (VEGFR-2), the matrix metalloproteases (MMP-2 and MMP-9), and thioredoxin reductase (TrxR1), where the complexes showed higher binding affinity in comparison to ligands, and particularly to auranofin, but comparable to sunitinib, an anti-angiogenic drug of clinical relevance.

Keywords: Gold(III) complexes, Phenanthroline, Cytotoxicity, Embryotoxicity, Angiogenesis

1. Introduction

Angiogenesis is a physiological process of the sprouting of new blood capillaries from preexisting vessels, which involves endothelial cells activation, invasion, migration, proliferation, tube formation and, finally, capillary network establishment [1]. While controllable and balanced angiogenesis play an essential role in normal physiological processes, an excessive activation of angiogenesis leads to numerous pathological processes, such as inflammatory disease, rheumatoid arthritis, psoriasis, artherosclerosis, diabetic retinopathy and cancer, for which growth, invasion and metastasis is crucial to form new vessels [2]. Accordingly, the blockade of angiogenesis by targeting activated endothelial cells and inhibiting them to proliferate and migrate is a proven strategy for the treatment of angiogenesis-related diseases [3]. It is evidenced that angiogenesis inhibitors combined with adjuvant chemotherapy increased its efficacy and provided significantly better survival of the cancer patients [4]. So far, more than 300 angiogenesis inhibitors have been developed, and 80 anti-angiogenic drugs are currently in clinical trials [5]. However, the drawbacks of many anti-angiogenic therapies, mostly associated with clinical resistance and toxicity, particularly cardiotoxicity [6], highlight the need for developing new drug candidates with improved bioactivity and a more favorable safety profile.

In recent years, the metal-based chemotherapeutics has undergone a renaissance, yet offering excellent and unexplored opportunities for further drug discovery [7]. In this vein, gold-based compounds present a very promising family of cytotoxic and potentially anticancer agents [8-10]. While many gold(III)-complexes containing organic heterocyclic ligands were proven for substantial anticancer activity [8,9], an anti-angiogenic activity has been demonstrated only for few of them including complexes with porphyrins, phenylpyridines, Schiff-base ligands [11-15] and, recently, with L-histidine-containing dipeptides [16]. One of the successful approaches in the anti-angiogenic gold(III)

complexes design might be relied on the use of ligands with proven anti-angiogenic activity, while keeping desired toxicological profiles.

An important class of ligands for the synthesis of gold(III) complexes comprises aromatic nitrogen-containing heterocycles (*N*-heterocycles), since they represent structural moieties of many natural products and biologically active compounds possessing diverse pharmacological properties, such as antitumor, antimicrobial, anticonvulsant, anti-inflammatory and anti-angiogenic [17-20]. Among these compounds, 1,10-phenanthroline (1,10-phen) has been the most extensively explored and frequently used owing to its planar structure, metal chelating properties, capability to bind to DNA by intercalation and cytotoxic activity against numerous cancer cell lines [21-29]. However, the previous studies revealed that 1,10-phen and the corresponding gold(III) complex, [Au(1,10-phen)Cl_2]Cl, had no selective activity against tumor cell lines in comparison to normal human and mammalian cell lines [22,24,26,27], whereas 1,10-phen exerted equal to or even higher cytotoxicity on cancer cell lines than the corresponding platinum(II) and gold(III) complexes [25,26]. Recently, Ellis and Crawford [20] found that 1,10-phen possesses ability to inhibit blood vessels development in zebrafish embryos, eliciting the toxic response in embryos upon an effective anti-angiogenic concentrations. All these biological properties limit the future application of 1,10-phen as a ligand for design and synthesis of metal-based anti-angiogenic drugs.

Owing to high molecular, genetic and physiological similarity between zebrafish and mammals, including humans, zebrafish emerged as reliable and very predictive high-throughput model system in early drug discovery process [30], enabling identification of molecules with potential therapeutic effect on the certain targets and elimination of those with toxic effect [31,32]. As the vascular system is highly conserved between zebrafish and mammals and requires the same necessary proteins for blood vessel growth, zebrafish

emerged also as a powerful platform for the identification of novel angiogenesis inhibitors [33,34].

Based on the discovery of anti-angiogenic property of 1,10-phen [20], and prompted by findings that phenanthrolines with differentially positioned nitrogen atoms, such as 1,7-phenanthroline (1,7-phen) and 4,7-phenanthroline (4,7-phen), are significantly less toxic, mutagenic and genotoxic than 1,10-phen [35,36], but nevertheless have not been used for the synthesis of gold(III) complexes, we decided to synthesize two new gold(III) complexes, [$AuCl_3$(1,7-phen-κ*N*7)] (**1**) and [$AuCl_3$(4,7-phen-κ*N*4)] (**2**). These complexes were characterized by NMR (^{1}H and ^{13}C), IR and UV-vis spectroscopic and single-crystal X-ray diffraction analysis. DFT calculations were employed in order to explain coordination mode of 1,7- and 4,7-phen toward the $AuCl_3$ fragment. Both phenanthroline ligands and gold(III) complexes were explored for their cytotoxic properties and the capabilities to inhibit the migration of endothelial cells *in vitro* and the angiogenesis *in vivo* in zebrafish (*Danio rerio*) embryos, which were also used for the toxicity assessment. Their anti-angiogenic activities have been compared to those of auranofin and sunitinib, the two drugs of clinical relevance and with anti-angiogenic properties. In addition, *in silico* study was performed to evaluate the potential of the gold(III) complexes and the corresponding phenanthroline ligands to bind some of the most important targets implicated in the process of angiogenesis such as vascular endothelial growth factor receptors (VEGFRs), the matrix metalloproteases (MMPs) and thioredoxin reductases (TrxRs).

2. Experimental

2.1. Materials

Distilled water was demineralized and purified to a resistance of greater than 10 MΩ·cm. Potassium tetrachloridoaurate(III) ($K[AuCl_4]$), 1,7-phenanthroline (1,7-phen), 4,7-phenanthroline (4,7-phen), ethanol, acetonitrile, dimethylformamide (DMF) and acetone-d_6 were purchased from the Sigma-Aldrich. All the employed chemicals were of analytical reagent grade and used without further purification.

2.2. Measurements

Elemental microanalyses of the synthesized gold(III) complexes for carbon, hydrogen and nitrogen were performed by the Microanalytical Laboratory, Faculty of Chemistry, University of Belgrade. All NMR spectra were recorded at 25 °C on a Bruker Avance III 400 MHz spectrometer. 5 mg of each compound was dissolved in 0.6 mL of acetone-d_6 and transferred into a 5 mm NMR tube. Chemical shifts are reported in ppm (δ) and scalar couplings are reported in Hertz. The IR spectra were recorded as KBr pellets on a Perkin Elmer Spectrum One spectrometer over the range 450 – 4000 cm^{-1}. The far-IR spectra were measured on a Perkin Elmer 983 spectrophotometer using Nujol mull supported between CsI sheets. The UV-vis spectra were recorded on a Perkin Elmer Lambda 35 double-beam spectrophotometer equipped with thermostated 1.00-cm quartz Suprasil cells after dissolving the gold(III) complexes **1** and **2** in DMF, over the wavelength range of 200 – 600 nm. The concentration of the gold(III) complexes was $2.5 \cdot 10^{-4}$ M.

*2.3. Synthesis of gold(III) complexes **1** and **2***

Gold(III) complexes, [$AuCl_3$(1,7-phen-κ*N*7)] (**1**) and [$AuCl_3$(4,7-phen-κ*N*4)] (**2**), were synthesized according to the modified procedure for the preparation of [$AuCl_3$(*N*-heterocycle)] complexes [37].

The solution of 0.25 mmol of the corresponding *N*-heterocyclic ligand (45.0 mg, 1,7-phen for **1** and 4,7-phen for **2**) in 5.0 mL of ethanol was added slowly under stirring to the solution containing an equimolar amount of K[$AuCl_4$] (94.5 mg in 5.0 mL of ethanol). The resulting yellow solution was stirred in the dark at ambient temperature for 5 h. The formed yellow precipitate was filtered off, washed with water and dissolved in acetonitrile. The obtained solution was left in a refrigerator and, after a few days, yellow crystals suitable for single-crystal X-ray crystallography were formed. These were filtered off and dried in the dark at ambient temperature. The yield was 63% for **1** (76.2 mg) and 54% for **2** (65.3 mg).

Anal. calcd. for **1** = $C_{12}H_8AuCl_3N_2$ (M_r = 483.52): C, 29.81; H, 1.67; N, 5.79. Found: C, 29.62; H, 1.85; N, 6.01%. ^{1}H NMR (400 MHz, CD_3COCD_3): δ = 7.98 (*dd*, *J* = 8.2, 4.4 Hz, H-4), 8.36 (*dd*, *J* = 8.2, 5.7 Hz, H-10), 8.70 (*d*, *J* = 9.4 Hz, H-3), 8.75 (*dd*, *J* = 8.2, 1.7 Hz, H-5), 8.89 (*d*, *J* = 9.3 Hz, H-9), 9.28 (*dd*, *J* = 4.4, 1.7 Hz, H-2), 9.83 (*dd*, *J* = 5.7, 1.4 Hz, H-8), 10.20 ppm (*d*, *J* = 8.2 Hz, H-6). ^{13}C NMR (101 MHz, CD_3COCD_3): δ = 123.78 (C-9), 124.85 (C-4), 125.12 (C-10), 126.66 (C-4a), 131.05 (C-10a), 134.69 (C-3), 137.08 (C-5), 139.37 (C-6), 143.96 (C-1a), 150.99 (C-6a), 151.97 (C-2), 152.80 ppm (C-8). IR (KBr, ν, cm^{-1}): 3078(m), 2921(m), 2852(w), 1614(s), 1601(s), 1515(m), 1497(s), 1435(s), 1417(w), 1399(m), 1296(s), 1259(w), 1231(w), 1107(m), 1051(w), 1001(w), 883(w), 858(w), 836(s), 830(s), 796(s), 786(vs), 723(w), 514(w). Far-IR (CsI, ν, cm^{-1}): 363(s), 340 (sh). UV-vis (DMF, λ_{max}, nm): 322.0 (ε = $4.0 \cdot 10^3$ $M^{-1}cm^{-1}$).

Anal. calcd. for **2** = $C_{12}H_8AuCl_3N_2$ (M_r = 483.52): C, 29.81; H, 1.67; N, 5.79. Found: C, 29.51; H, 1.66; N, 6.05%. ^{1}H NMR (400 MHz, CD_3COCD_3): δ = 8.00 (*dd*, *J* = 8.5, 4.4 Hz, H-10), 8.37 (*dd*, *J* = 8.4, 5.7 Hz, H-1), 8.73 (*d*, *J* = 9.5 Hz, H-6), 9.08 (*d*, *J* = 9.6 Hz, H-5), 9.25 (*dd*, *J* = 4.4, 1.5 Hz, H-9), 9.47 (*d*, *J* = 8.3 Hz, H-8), 9.82 (*dd*, *J* = 5.7, 1.2 Hz, H-2), 9.94 ppm (*d*, *J* = 8.4 Hz, H-3). ^{13}C NMR (101 MHz, CD_3COCD_3): δ = 123.96 (C-10), 124.98 (C-1), 125.47 (C-10a), 126.88 (C-5), 131.05 (C-1a), 132.16 (C-8), 137.00 (C-6), 138.57 (C-3), 147.49 (C-6a), 149.52 (C-4a), 152.05 (C-2), 152.96 ppm (C-9). IR (KBr, ν, cm^{-1}): 3077(w), 3058(w), 3039(w), 3005(w), 2965(w), 1582(m), 1527(w), 1498(vs), 1450(m), 1410(m), 1389(w), 1341(w), 1300(s), 1263(w), 1112(w), 1060(w), 825(s), 803(s), 751(w), 565(w), 541(w). Far-IR (CsI, ν, cm^{-1}): 359(s), 342 (sh). UV-vis (DMF, λ_{max}, nm): 321.0 ($\varepsilon = 3.6 \cdot 10^3$ $M^{-1}cm^{-1}$).

2.4. Crystallographic data collection and refinement of the structures

Crystal data for **1** and **2** are provided in Table S1. Intensity measurements have been carried out on XCALIBUR diffractometer equipped with Mo X-ray tube and graphite monochromator [38]. Crystals of **2** appeared to be twinned and this has been accounted for by the "Twinning – multi-crystals" procedure implemented into the CrysAlis program [38]. In addition to the routinely applied absorption corrections, semiempirical absorption corrections were performed for **1**. An analogous absorption correction for the X-ray data for **2** appeared difficult to apply, for this data set has already been subjected to the untwining procedure. Following structure solution with SHELXT [39], positional parameters and anisotropic temperature factors were refined against F^2 with SHELXL [40]. Hydrogen atoms were included at calculated sites with U values equal to 1.2 times the value of the equivalent isotropic temperature factor of the parent C atom.

2.5. Quantum-mechanical methods

The M06-2X functional in combination with the conductor-like solvation model CPCM [41] was used to optimize the geometries and to perform the frequency calculations of the examined systems in the ethanol solution (dielectric constant of ethanol at 298.15 K is 24.852). In all calculations the LanL2TZ(f) basis set for the gold and cc-pVTZ basis set for all other atoms were employed. These calculations were performed using the Gaussian 09 program package [42].

The dual descriptor can give information about the ability of a molecule to donate/accept electrons in a given chemical reaction [43,44]. Positive values of the dual descriptor correspond to electrophilic regions, while negative ones correspond to nucleophilic regions in a molecule. In the case of planar molecules, σ- and π-electrons give clearly distinguishable contributions to the calculated electronic densities. In the present work, the σ- and π-contributions of the dual descriptor were employed. Calculations of dual descriptors were performed using our own Fortran routines requiring as input formatted checkpoint files from Gaussian 09.

2.6. Evaluation of cytotoxicity by MTT assay

Cytotoxicity in terms of the antiproliferative effect was tested by the 3-(4,5-dimethylthiazol-2-yl)-2,5-diphenyltetrazolium bromide (MTT) assay [45]. The assay was carried out using human lung fibroblasts (MRC5), human cervix cancer (HeLa), lung cancer (A549) and human immortalized endothelial-like EA.hy926 cell lines after 48 h of cell incubation in the medium, containing compounds at concentrations ranging from 0.25 to 200 μM. Briefly, MRC5, HeLa and A549 cells were maintained in RPMI-1640 medium supplemented with 100 μg/mL streptomycin, 100 U/mL penicillin and 10% (v/v) fetal bovine serum (FBS) (all from Sigma, Munich, Germany) as a monolayer (1×10^4 cells per

well). EA.hy926 cell line was maintained in Dulbecco's Modified Eagle's medium (DMEM) supplemented with 10% fetal bovine serum (FBS) and HAT supplement (Gibco-BRL) as a monolayer (1×10^4 cells per well). All cell lines were grown in humidified atmosphere of 95% air and 5% CO_2 at 37 °C. The MTT assay was performed two times in four replicates. The extent of MTT reduction was measured spectrophotometrically at 540 nm using a Tecan Infinite 200 Pro multiplate reader (Tecan Group Ltd., Männedorf, Switzerland), and the cell survival was expressed as percentage of the control (untreated cells). Cytotoxicity was expressed as the concentration of the compound inhibiting cell growth by 50% (IC_{50}) in comparison to untreated control.

2.7. Wound-scratch migration assay

EA.hy926 cells (3×10^5) were cultured as confluent monolayers in DMEM supplemented with 10% FBS, synchronized in 1% FBS for 24 h and wounded by removing a 300- to 500 μm-wide strip of cells across the well with a standard 200 μL pipette tip [46]. Wounded monolayers were washed twice with phosphate-buffered saline (PBS) to remove non-adherent cells and then treated with 200 μM gold(III) complexes **1** and **2**, the respective phenanthroline ligands and $K[AuCl_4]$, as well as with 5 μM auranofin for 6 h. EA.hy926 cell migration into the wounded area was photographed at the indicated times at the same spot with an DM IL LED Inverted Microscope equipped with a digital camera (Leica Microsystems, Wetzlar, Germany). The extent of healing was defined as the ratio of the difference between the original and the remaining wound areas compared with the original wound area. The closure of the gap distance was quantified using Leica Application Suite V4.3.0 (Leica Microsystems).

2.8. Embryotoxicity and anti-angiogenic potential evaluation in zebrafish model

Assessment of toxicity and anti-angiogenic activity of gold(III) complexes on zebrafish embryos model was carried out according to general rules of the OECD Guidelines for the Testing of Chemicals [47]. All experiments involving zebrafish were performed in compliance with the European directive 86/609/EEC and the ethical guidelines of the Guide for Care and Use of Laboratory Animals of the Institute of Molecular Genetics and Genetic Engineering, University of Belgrade.

Adult zebrafish (*Danio rerio*, wild type) were obtained from a commercial supplier (Pet Center, Belgrade, Serbia), housed in a temperature- and light-controlled facility with 28 °C and standard 14:10-hour light-dark photoperiod, and regularly fed with commercially dry flake food (TetraMin^{TM} flakes; Tetra Melle, Germany) twice a day and *Artemia nauplii* once daily. Zebrafish embryos were produced by pair-wise mating, collected and distributed into 24-well plates containing 10 embryos per well and 1 mL embryos water (0.2 g/L of Instant Ocean® Salt in distilled water), and raised at 28 °C. For assessing lethal and developmental toxicity, embryos at 6 hours post fertilization (hpf) stage were treated with eight concentrations of gold(III) complexes **1** and **2**, $K[AuCl_4]$, 1,7- and 4,7-phen (2.5, 5, 10, 20, 40, 60, 80 and 100 μM), and five concentrations of auranofin (1.25, 2.5, 5, 7.5 and 10 μM). DMF (0.035%) and DMSO (0.1%) were used as negative controls. Experiments were performed three times using 20 embryos per concentration.

Apical endpoints for the toxicity evaluation (Table S2) were recorded at 24, 48, 72, 96 and 114 hpf using an inverted microscope (CKX41; Olympus, Tokyo, Japan). Dead embryos were counted and discarded every 24 h. At 114 hpf, embryos were inspected for heartbeat rate, anesthetized by addition of 0.1% (w/v) tricaine solution (Sigma-Aldrich, St. Louis, MO), photographed and killed by freezing at -20 °C for ≥ 24 h.

Anti-angiogenic potential of tested compounds was assessed using transgenic zebrafish embryos *Tg*(*fli1:EGFP*) expressing enhanced green fluorescent protein (EGFP) in endothelial cells. Embryos of *Tg*(*fli1:EGFP*) zebrafish were kindly provided by Dr. Ana Cvejic (Wellcome Trust Sanger Institute, Cambridge, UK) and raised in our zebrafish facility to adult stage under previously described life conditions. Transgenic embryos used in this assay were generated by natural spawning of wild type and *Tg*(*fli1:EGFP*) adults and reared in embryo water at 28 °C. Embryos staged at 20 hpf were dechorionated with fine tweezers immediately prior to drug treatment, arrayed in 24-well plate with 10 embryos per well, and incubated with 1 mL of embryo water per well containing various concentration of drugs (2.5, 5, 10, 17.5 µM) at 28 °C. 0.035% DMF was used as negative control. After drug treatments, zebrafish embryos were anesthetized with 0.003% tricaine (Sigma-Aldrich) and subsequently photographed. The intersegmental blood vessels (ISVs) and subintestinal vessel plexus (SIVs) development were inspected and imaged in embryos at 48 and 72 hpf, respectively under a fluorescence microscope (Olympus BX51, Applied Imaging Corp., San Jose, CA, USA). Auranofin (Sigma-Aldrich) and sunitinib (Sutent, Pfizer, New York) were used as positive controls with known anti-angiogenic activity [48,49].

2.9. Toxicity and angiogenesis parameters

Toxicity was evaluated by determination of the lethal concentration (LC_{50}), which was the treatment concentration resulting in 50% mortality of the embryos over a period of 114 hpf, and the effective concentration (EC_{50}) that is the treatment concentration affecting 50% embryos (lethal and teratogenic outcomes). In order to characterize teratogenic potential of the tested substances, the teratogenicity index (TI) was determined. TI was calculated as the ratio of LC_{50} and EC_{50}. Anti-angiogenic activity was evaluated by

determination of anti-angiogenic concentration (IC_{50}), which was the treatment concentration resulting in anti-angiogenic phenotype at 50% of embryos. To address anti-angiogenic potential, the therapeutic window (TW), as the ratio of LC_{50} and IC_{50} was determined. Determination of LC_{50}, EC_{50} and IC_{50} values was performed by the program ToxRatPro (ToxRat®, Software for the Statistical Analysis of Biotests, ToxRat Solution GmbH, Alsdorf, Germany, Version 2.10.05) using probit analysis with linear maximum likelihood regression.

2.10. Molecular docking study

The protein structures of matrix metalloprotease-2 (MMP-2; pdb code 1HOV, model 1), matrix metalloprotease-9 (MMP-9; pdb code 1GKC), human thioredoxin reductase (TrxR1; pdb code 2ZZ0) and vascular endothelial growth factor receptor (VEGFR-2; pdb code 3VHE) were extracted from Protein Data Bank, and used for docking study as targets for the tested compounds. The preparation of enzyme structure included the adding hydrogen atoms, removing water molecules and other ligands and ions from crystal structure (in MMPs both zinc ions were retained). In order to find binding sites and clarify the nature of interactions between tested compounds and targeted protein, molecular docking computations have been carried out using AutoDock 4.2 software program [50]. The structures of the tested compounds were optimized at the M06-2X/cc-pVTZ+LanL2TZ(f) level of theory, while the atomic charges were calculated at same level, according to the Merz–Kollman scheme *via* the restrained electrostatic potential (RESP) model [51]. For zinc ions from proteins formal charge of +2 was used. All hydrogen atoms were added to the proteins. Optimized structures of the tested compounds and structures of the proteins were used to generate grid and docking parameter files in AutoDockTools program [50]. The rotatable bonds of tested compounds were allowed to

rotate freely, while the structure of protein was considered rigid. A grid box, containing the whole protein, was used to accommodate the tested compounds to move freely during docking study. AutoDock virtual screening used 10 runs for each docking experiment with Lamarckian genetic algorithm as the search method. The results of docking studies were analyzed and visualized using Discovery Studio, BIOVIA Software product [52].

3. Results and Discussion

*3.1. Synthesis and structural characterization of **1** and **2***

Two aromatic *N*-heterocycles, 1,7-phenanthroline (1,7-phen) and 4,7-phenanthroline (4,7-phen), were used as ligands for gold(III) complexes (Fig. 1A). The two ligands have different steric and electronic properties and are likely to form complexes of different nuclearity. Steric considerations suggest that only monodentate κ*N7* coordination is to be expected for 1,7-phen, while nonlinear μ-*N4,N7* bridging should be possible for 4,7-phen [53]. All reactions were performed by mixing the reactants in different molar ratios (n($[AuCl_4]^-$) : n(x,7-phen) = 1 : 1 and 2 : 1, respectively) at room temperature in ethanol. Although the investigated *N*-heterocycles possess benzene spacer between two pyridine rings, their reactions with $[AuCl_4]^-$ invariably lead to the formation of mononuclear gold(III) complexes, $[AuCl_3$(1,7-phen-κ*N7*)] (**1**) and $[AuCl_3$(4,7-phen-κ*N4*)] (**2**), having one monodentatedly coordinated *N*-heterocyclic ligand. The stoichiometries of **1** and **2** were confirmed by elemental microanalysis, and the structures were elucidated by NMR (^{1}H and ^{13}C), IR and UV-vis spectroscopic and single-crystal X-ray diffraction analyses. DFT calculations were conducted to provide better insight into the coordination mode of 1,7- and 4,7-phen toward the $AuCl_3$ fragment.

3.1.1. Description of the single crystal structures

As depicted in Fig. 1B, the investigated complexes contain Au(III) ion coordinated in a square-planar fashion by three chloride anions and nitrogen from C_s symmetrical 1,7-phenanthroline (N7) and C_{2v} symmetrical 4,7-phenanthroline (N4). Although similar in a formal sense, the monodentate coordination of 1,7- and 4,7-phen ligands to the $AuCl_3$ core leads to notably different molecular and crystal structures, *e.g.* mutual orientation of $AuCl_3$ and phenanthroline moieties is nearly perpendicular (83.15(4)°) in **1** and more inclined (74.52(9)°) in **2**, and the Au-Cl bonds are more diverse in **1** and more equalized in **2** (Table S3).

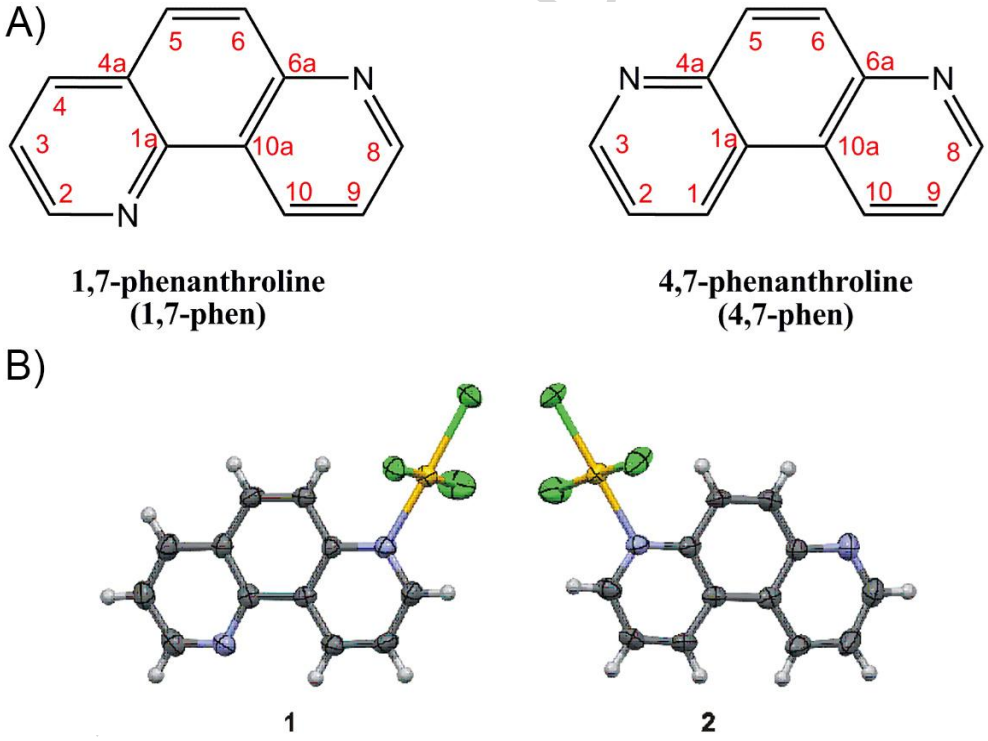

Fig. 1. (A) Schematic drawing of 1,7- and 4,7-phenanthroline ligands. The numeration of carbon atoms is in agreement with IUPAC recommendations for fused ring systems. (B) Molecular structures of [$AuCl_3$(1,7-phen-κ*N*7)] (**1**) and [$AuCl_3$(4,7-phen-κ*N*4)] (**2**) complexes. Thermal ellipsoids are drawn at 50% probability level. H-atoms are represented in an arbitrary scale.

Diversity of the Au-Cl bond lengths in **1** presumably steams from the exceptionally rich variety of intermolecular interactions including Au···Cl, Cl···Cl, columnar stacking, numerous C-H···Cl, as well as C-H···N hydrogen bonds. Geometrical parameters describing these interactions are listed in Table S4 and depicted in Fig. 2. Compared to the crystals of **1**, in the crystals of **2**, both Au···Cl and Cl···Cl contacts are longer (Table S4), so these molecules are more loosely packed, which is reflected in the density values for the two crystals and in the values of packing parameters listed in Table S1. The more easy approach to the uncomplexed nitrogen atom N7 in **2** compared to the uncomplexed nitrogen atom N1 in **1** is reflected in much more favorable intermolecular C-H···N hydrogen bond parameters listed in Table S4.

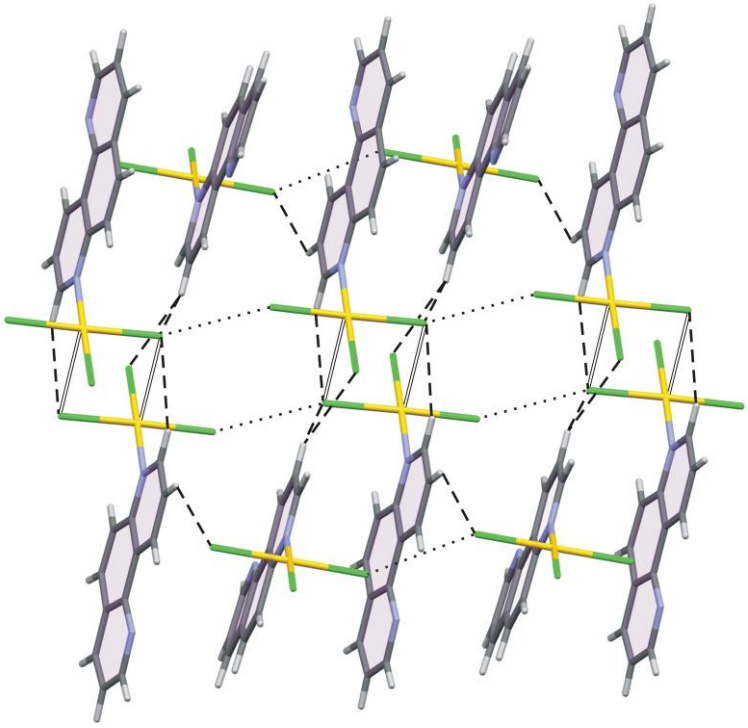

Fig. 2. Diversity of intermolecular interactions in the crystal structure of **1**. H-bonds: dashed lines; Au···Cl: open lines; Cl···Cl: dotted lines; face-to-face stacking: shaded areas.

3.1.2. Spectroscopic characterization

The NMR (^{1}H and ^{13}C), IR and UV-vis spectroscopic data for gold(III) complexes **1** and **2** are listed in the section 2.3 (*vide infra*) and are consistent with the structures determined by single-crystal X-ray analysis. The ^{1}H NMR spectra of the gold(III) complexes **1** and **2** were noticeably different from those of uncoordinated 1,7- and 4,7-phen ligands. Monodentate coordination to Au(III) ion caused a desymmetrization of the ligands, resulting in appearance of eight proton signals in the spectra of complexes (instead of five and four proton signals in the spectra of uncoordinated 1,7- and 4,7-phen, respectively). The position of 1,7-phen ligand coordination (bonding to which of the two different nitrogen atoms, N1 or N7) was deduced from the largest values of the observed coordination shifts (determined in respect to the free ligand) in the ^{1}H spectrum of the corresponding gold(III) complex **1**. $\mathbf{\Delta}(^{1}H)_{coord}$ values confirmed that this ligand is coordinated to Au(III) *via* the nitrogen atom N7: $\mathbf{\Delta}(^{1}H)_{coord}$ was the highest (*c.a.* 0.8 ppm) for H-8, while the coordination shift for its counterpart, H-2, was significantly lower (*c.a.* 0.2 ppm). The auration of 1,7- and 4,7-phen resulted in an overall ^{1}H deshielding, what can be ascribed to a delocalization of the charge deficiency (cation formation (N^{+}) by electron-withdrawing $AuCl_3$ group coordination) throughout the rings of the ligands [54,55]. Although on the whole, Au(III) complexation of the ligands produced an overall deshielding of ring carbons in complexes **1** and **2**, the signals of several carbon atoms were shifted upfield.

The IR spectra of the complexes **1** and **2** recorded in the range of 4000 – 450 cm^{-1} show the peaks that are atrributed to the coordinated phenanthroline ligands. In the Far-IR region, the most obvious feature is the very strong band at 363 and 359 cm^{-1} for **1** and **2**, respectively, which can be assigned to the antisymmetric stretching vibration of Au–Cl bond, which is in the *trans* position in respect to the coordinated nitrogen atom. This is in

accord with the previous IR study of a series of gold(III) complexes of the general formula [$AuCl_3L$], L stands for pyridine, 2-, 3- and 4-methylpyridine, 2,6-, 3,5- and 2,4-lutidine and 4-cyanopyridine, where it was assumed that the strong band in the range of 366 – 356 cm^{-1} was due to the antisymmetric stretching vibration of the *trans* Au–Cl bond [56]. Moreover, shoulder at 340 and 342 cm^{-1} in the Far-IR spectra of **1** and **2**, respectively, can be tentatively assigned to the symmetric stretching vibration of this bond, as it was found previously for the abovementioned [$AuCl_3L$] complexes [56], in which spectra, very week and difficult to identify band due to this vibration was observed in the range of 345 – 333 cm^{-1}.

The shape of the UV-vis spectra and values of λ_{max} are almost identical for both of complexes (λ_{max} = 322.0 and 321.0 nm for **1** and **2**, respectively) confirming the same (monodentate) coordination mode of the phenanthroline ligands in **1** and **2**. The absorbance peaks for **1** and **2** show significant red shifts compared to those for the uncoordinated *N*-heterocycles (λ_{max} = 267.0 and 270.0 nm for 1,7- and 4,7-phen, respectively), indicating that the absorption observed for the complexes can be attributed to LMCT (ligand-to-metal charge transfer) transitions [57].

3.2. Theoretical studies

The structures of the mononuclear gold(III) complexes **1** and **2**, were optimized in the ethanol at the M06-2X(CPCM)/cc-pVTZ+LanL2TZ(f) level of theory. The optimized geometries of **1** and **2** are shown in Fig. S1, and the values of the calculated bond lengths and bond angles are given in Table S3. It can be seen that the calculated bond lengths and angles are in very good agreement with the corresponding X-ray structural data. This supports our recently obtained results showing that the M06-2X method provides an appropriate prediction of the crystal structure parameters of the gold(III) complexes with

aromatic *N*-heterocycles [55,57]. In addition, the M06-2X functional has been successfully applied to study the electron-donating properties of aromatic *N*-heterocycles [58].

Considering the fact that 1,7-phen ligand contains two potential metal binding nitrogens with different environment, two possible mononuclear complexes that can be obtained in its reaction with $[AuCl_4]^-$, $[AuCl_3(1,7\text{-phen-}\kappa N1)]$ and $[AuCl_3(1,7\text{-phen-}\kappa N7)]$, were subjected to DFT calculations. The structures of these gold(III) complexes and their relative free energies calculated at the M06-2X(CPCM)/cc-pVTZ+LanL2TZ(f) level of theory are given in Fig. 3A. As can be seen from the relative free energies, the coordination of Au(III) ion to the nitrogen atom N7 is thermodynamically more favorable than the coordination to N1. This goes along the fact that the coordination of Au(III) to N1 is followed by a loss of planarity in the aromatic 1,7-phen ligand. Besides that, the isodensity surfaces of the dual descriptor, that is very useful in prediction of the sites of electrophilic and nucleophilic attack, and its σ- and π-orbital contributions for the free 1,7-phen ligand were examined (Fig. 3B-D). From the dual descriptor isodensity surface (Fig. 3B), it is not clear how to differentiate nucleophilic character of the two nitrogen atoms in 1,7-phen. Bearing in mind that 1,7-phen coordination to the Au(III) ion goes through σ lone pair of nitrogen, it is more reasonable to explore the σ-orbital dual descriptor isodensity surface. Fig. 3C clearly shows that N7 has more pronounced nucleophilic character than N1. This result implies that, beside steric, electronic effects also govern the coordination of Au(III) ion to N7 nitrogen.

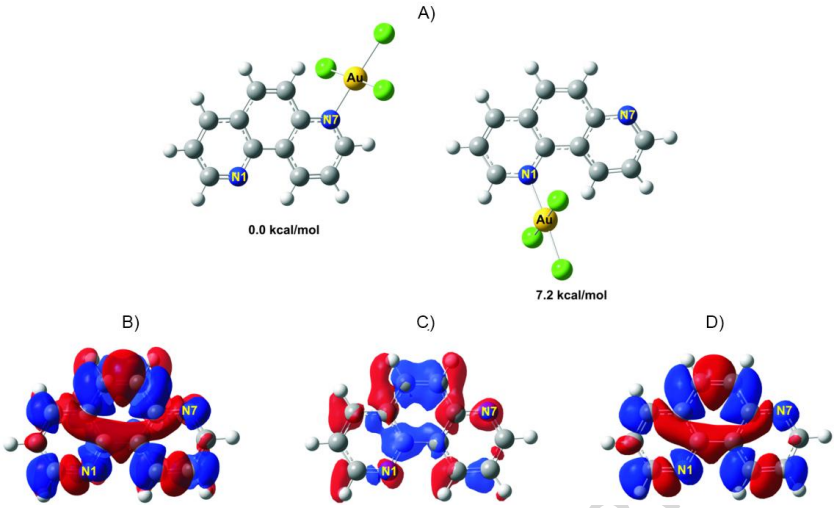

Fig. 3. (A) The structures of two possible mononuclear gold(III) complexes, [$AuCl_3$(1,7-phen-κ*N*7)] and [$AuCl_3$(1,7-phen-κ*N*1)], and their relative free energies calculated at the M06-2X(CPCM)/cc-pVTZ+LanL2TZ(f) level of theory. Dual descriptor isovalue surface (0.001 a.u.) for 1,7-phen: total (B), σ-orbital contribution (C) and π-orbital contribution (D). Nucleophilic and electrophilic regions are colored in red and blue, respectively.

A detailed mechanistic study of the formation of mononuclear complexes **1** and **2** and their hypothetic dinuclear analogues, {[$AuCl_3$]$_2$(μ-1,7-phen)} and {[$AuCl_3$]$_2$(μ-4,7-phen)}, was performed (Figs. S2 and S3, and Table S5). It was shown that the formation of the mononuclear complexes is thermodynamically and kinetically favored over the formation of their dinuclear analogues, being in line with the experimental results (Fig. S4).

3.3. Cytotoxicity and cell-migration

The cytotoxic effect of complexes **1** and **2** in the healthy human fibroblasts and several cancer cell lines was between 1.1 and 2.1-fold higher in comparison to 1,7- and 4,7-phen (Table 1). This slightly improved cell-killing effects of the complexes in comparison to the respective ligands can be attributed to the presence of gold(III) center. However, the cytotoxic effect of both gold(III) complexes and phenanthrolines was much lower in

comparison to that of auranofin and comparable or higher in comparison to that of $K[AuCl_4]$. None of the tested compounds exhibited significant selectivity between healthy MRC5 and cancer cell lines (Table 1). The cytotoxic potential of auranofin was confirmed, with IC_{50} values in accordance to the previous studies on the same or similar cell lines [59]. Phenanthrolines used in this study (Fig. 1A), although structurally similar to 1,10-phenanthroline, showed between 5- and 50-fold reduced cytotoxic effect in comparison to 1,10-phen against cisplatin-sensitive breast (MCF-7) and resistant ovarian (SKOV-3) cancer cell lines and A2780 ovarian cell line either sensitive or resistant to cisplatin [26,60]. For 1,10-phenanthroline, it has been hypothesized that the biological effects are due to its metal chelating properties [61,62]. To our best knowledge, the cytotoxic properties of 1,7- and 4,7-phen have not been reported previously, however it is apparent that different position of nitrogen atoms results in much lower cytotoxicity.

The low *in vitro* cytotoxic effect of **1** and **2** is in line with our recent observation of the low cytotoxicity of gold(III) complexes with L-histidine-containing dipeptides [16]. Similarly, mononuclear gold(III) complexes containing various *N*-heterocycles (pyridazine, pyrimidine, pyrazine, quinoxaline and phenazine) were shown to have moderate to low cytotoxicity, but pronounced ability to intercalate double stranded DNA *in vitro* [63].

Overall, gold(III)-phenanthroline complexes **1** and **2** did not show pronounced cytotoxic nor anticancer potential, however their low cytotoxicity towards normal cell line made them suitable candidates for further examination towards the other biological activities. Prompted by the our recent study showing good anti-angiogenic potential of gold(III) complexes with L-histidine-containing dipeptides [16], we have decided to evaluate the anti-angiogenic potential of the gold(III) complexes **1** and **2**. Considering that the cell migration is necessary for endothelial angiogenesis, as well as for cancer cell invasion and

metastasis, we have firstly performed classical scratch wound healing assay in human immortalized endothelial-like cell line EA.hy926 to determine the antimigratory effects of gold(III) complexes **1** and **2**. Cells were treated with concentrations corresponding to double IC_{50} values of compounds (Table 1), and the migration of the cells into the wound area was monitored throughout a 6 h time window (Fig. 4). Under the tested conditions, the best antimigratory effects were observed upon treatment with complex **1** and 1,7-phen. In comparison to the migration rate of EA.hy926 cells without drug treatment, the wound closure effects for complex **1** and 1,7-phen were reduced to 42 and 47%, respectively. Complex **2** showed antimigratory effect comparable to that of auranofin. The EA.hy926 cells incubated with 4,7-phen and $K[AuCl_4]$ migrated to approximately same extent as control cells within the same time window. Interestingly, quite different activity of two phenanthrolines was observed in this test, suggesting some specific inhibition caused by the difference in the position of nitrogen atoms (Fig. 1A). Indeed, the cells treated with 1,7-phen showed different more rounded morphology from those upon 4,7-phen treatment (Fig. 4B), and the change of the cell shape was reported to influence the cell motility [64]. Auranofin expectedly showed inhibitory effect against wound-healing, in accordance with the previously reported study of its anti-angiogenic effect on human umbilical vein endothelial cells (HUVEC) [49]. The presented results indicate that both gold(III)-phenanthroline complexes could influence the migration capability of endothelial cells.

Table 1

Cytotoxic activity expressed as IC_{50} value (μM) for gold(III) complexes **1** and **2** in comparison to that for 1,7- and 4,7-phenanthroline, $K[AuCl_4]$ and clinically used drug auranofin, upon treatment for 48 h.

Cell line / Compound	IC50 (μM)[a]			
	MRC5	**HeLa**	**A549**	**EA.hy926**
$[AuCl_3$(1,7-phen-κ*N*7)$]$ (1)	80±4	62.5±2	70±3	100±5
1,7-phen	135±14	70±4	150±10	120±7
$[AuCl_3$(4,7-phen-κ*N*4)$]$ (2)	120±5	115±8	85±2	130±6
4,7-phen	170±9	125±5	155±6	140±8
$K[AuCl_4]$	150±12	170±4	160±8	165±5
Auranofin	0.5±0.02	0.5±0.04	0.5±0.01	2.5±0.1

[a]IC_{50} is defined as the concentration inhibiting 50% of cell growth after the treatment with the test compounds. Results are from two independent experiments, each performed in quadruplicate, represented as mean ± SD.

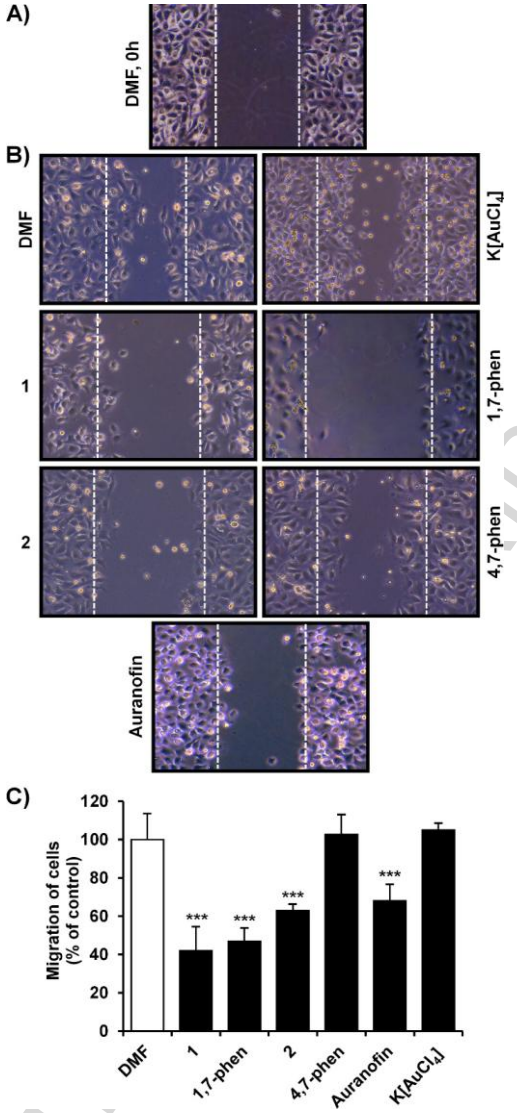

Fig. 4. Wound healing migration of EA.hy926 cells. Effects of gold(III) complexes **1** and **2**, phenanthroline ligands and $K[AuCl_4]$, applied in concentration of 200 µM, on the migration of EA.hy926 cells after treatment for 6 h (B) in comparison to solvent (DMF) control at time 0 h (A). Auranofin (5 µM) was used as reference anti-angiogenic compound. For each treatment condition, eight measurements were taken randomly in each well. Data are presented as mean ± SD of two independent experiments with * $P < 0.05$; ** $P < 0.01$; *** $P < 0.001$ according to one-way ANOVA followed by the Bonferonni comparison test (C).

3.4. Embryotoxicity and anti-angiogenesis potential

In vivo toxicity assessment performed in this study on zebrafish embryos revealed that gold(III) complexes **1** and **2** were less toxic (both in terms of lethality and teratogenicity) than the respective phenanthroline ligands, and markedly less toxic than anti-angiogenic compounds auranofin and sunitinib (Fig. 5), ranking them according to toxicity, as follows: sunitinib > auranofin > 4,7-phen > 1,7-phen > $K[AuC1_4]$ > **2** > **1**. According to the determined LC_{50} values, gold(III) complexes **1** and **2** were 35- and 13-fold less toxic in comparison to auranofin, 118- and 45-fold less toxic than sunitinib, and 1.3- and 3-fold less toxic in comparison to the respective ligands. Notably, gold(III)-phenanthroline complexes showed neither developmental nor cardiovascular toxicity (pericardial edema and disturbed heartbeat rate) in zebrafish embryos in tested concentrations range of 2.5 – 100 μM, where the embryos survival was affected only at doses ≥ 80 μM of **1** and ≥ 40 μM of **2** (Fig. 5). Contrary to the complexes, phenanthroline ligands caused teratogenic defects in embryos at the concentrations ≥ 40 μM, such as the multiple edemas (pericardial sac, egg yolk sac and body) and skeletal deformities (reduced growth, malformed head and eyes, lordosis), similarly to defects following auranofin and sunitinib treatments at doses ≥ 1.25 μM. Results of the embryotoxicity of auranofin (Fig. 5) and sunitinib (data not shown) are in accordance with the previous studies on zebrafish embryo model [16,48]. These two clinically used drugs were found to cause the progressive cardiotoxicity (pericardial edema and decreased heartbeat rate) and skeletal deformities (reduced growth, malformed head and eyes, lordosis) already at concentration of 1.25 μM. $K[AuC1_4]$ complex had no effect on zebrafish development and showed higher embryotoxicity in comparison to gold(III) complexes **1** and **2**, but lower than that of phenanthroline ligands (Fig. 5).

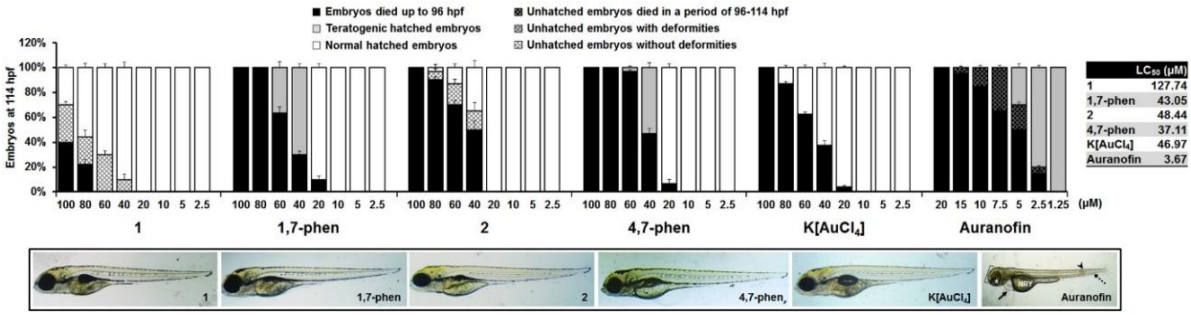

Fig. 5. Toxicity assay on zebrafish embryos exposed to gold(III) complexes **1** and **2**, ligands 1,7- and 4,7-phen, $K[AuCl_4]$ and auranofin expressed as LC_{50} values (μM). Morphology of zebrafish embryos at 114 hpf after treatment with 20 μM of **1**, **2**, ligands and $K[AuCl_4]$ (normal), and 1.25 μM of auranofin (teratogenic) are shown. Embryos upon auranofin treatment were retarded in the growth, had small or malformed head (bracket) and eyes (asterisk), large pericardial edema (arrow), non-resorbed egg yolk (NRY), signs of the tail lordosis (dashed arrow) and the necrotic tissue in the tail region (arrowhead).

To the best of our knowledge, the *in vivo* toxicity of 1,7- and 4,7-phen has not been addressed previously in the zebrafish embryos model. Recently, Ellis and Crawford [20] examined the embryotoxicity of 1,10-phen and reported the same teratogenic defects in embryos upon 5 μM as we observed upon eight times higher concentration of 1,7- and 4,7-phen. This suggests that 1,7- and 4,7-phen are less toxic than 1,10-phen, what has also been observed in cell-killing assays (Table 1), and may serve as suitable ligands for the metal complexes when activities other than antitumor are important.

From the comparison of embryotoxicity profiles of gold(III)-phenanthroline complexes with gold(III) complexes with L-histidine-containing dipeptides and other aromatic nitrogen-containing heterocycles, previously assessed in zebrafish embryo model [16,63], it can be concluded that the nature of ligands decisively determines the toxicity response in embryos (survival, cardiotoxicity and teratogenicity). According to LC_{50} values, the 1,7-

phenanthroline-containing complex **1** has stood out as the least toxic complex among all gold(III) complexes tested so far in zebrafish embryos model, with LC_{50} value of 128 μM.

Interestingly, it has been observed that gold(III) complexes **1** and **2**, but not the corresponding ligands, interfered with embryos hatching, like auranofin, but with different outcome (Fig. 5). While auranofin-treated embryos have already been prevented for hatching at 2.5 μM and died up to 114 hpf (hours post fertilization), the unhatched embryos occurring at 40 – 100 μM concentrations range of **1** and **2** survived up to 114 hpf. The hatching of zebrafish embryos is the process mainly driven by Zn-metalloproteases, which activity may be affected by diverse metal ions due to their binding to the enzyme's active site or by sequestering of Zn(II) ions by chelating compounds [65]. Hatching interference has already been reported upon exposure of embryos to gold(III) complexes with aromatic nitrogen-containing heterocycles and L-histidine-containing dipeptides [16,63], but the mechanism still needs to be elucidated.

It is important to emphasize that embryos following the treatment with gold(III)-phenanthroline complexes **1** and **2**, and the respective ligands showed reduced or absent caudal circulation, similarly to the pattern observed in embryos upon auranofin and sunitinib treatments. However, complex- and ligand-treated embryos did not have the body tissue necrosis, which has been developed upon the treatments with auranofin and sunitinib (Fig. 5).

Prompted by studies that showed inhibition of angiogenesis caused by auranofin and selection of gold(I) and gold(III) complexes [16,49,66] in combination with the observed pattern of reduced caudal circulation during the embryotoxicity assessment, we have decided to examine in detail the potential of gold(III) complexes **1** and **2** and the corresponding phenanthroline ligands to affect angiogenesis *in vivo* in the zebrafish model. The suppression effect on angiogenesis by complexes **1** and **2** has been studied using

transgenic zebrafish [*Tg*(*fli-1*:*EGFP*)] embryos, in which the endothelial cells expressing EGFP can be directly observed by fluorescence microscope. The developmental angiogenesis in zebrafish embryos, leading to the formation of the intersegmental vessels (ISVs) at 48 hpf, and subintestinal vessels (SIVs) at 72 hpf, represents a valuable target for the screening of anti-angiogenic compounds. Anti-angiogenic phenotype was defined as the reduced number/length of subintestinal vessels (SIVs) or intersegmental vessels (ISVs) along the whole body (normally 5 – 9 arcades in the SIV basket-like structure and 28 – 30 ISVs was developed), or as disrupted dorsal lateral vessels (DLAVs). Embryos were exposed to different doses of gold(III) complexes **1** and **2**, the corresponding phenanthroline ligands and $K[AuCl_4]$, that were previously determined not to cause the effect on embryonal development (Figs. 6, S5 and S6, Table S2). The obtained results revealed that both gold(III) complexes and the respective ligands are efficient anti-angiogenic compounds, while $K[AuCl_4]$ induced a negligible effect on the vessel development compared to the DMF (solvent vehicle)-treated group ($P > 0.05$, X^2 test). Complexes **1** and **2** were significantly more active than the respective ligands, with the anti-angiogenic phenotype observed at concentration of 2.5 μM of complexes and ≥ 10 μM for 1,7- and 4,7-phen (Figs. 6B and S5, Table S6). Overall, **1** and **2** achieved the similar rate of ISVs and SIVs angiogenesis inhibition as the respective ligands applied in 4- to 8-fold lower concentrations (Figs. 6 and S6, Table S6).

When comparing anti-angiogenic effects of **1** and **2** to the clinically relevant auranofin and sunitinib, it was observed that gold(III)-phenanthroline complexes applied in dose of 2.5 μM, achieved the same or higher inhibitory effects on ISVs angiogenesis in zebrafish embryos compared to 1.25 μM auranofin and sunitinib, which decreased the ISVs and SIVs length 33 and 59%, respectively, but caused serious pericardial edema and decreased the heart beating rate of treated embryos (Fig. S6, Table S6). When applied at the highest

tested dose of 20 μM, overall anti-angiogenic effect of **1** and **2** (the number of incomplete ISVs and the decrease in ISVs and SIVs length) was higher than that of 1.25 μM of sunitinib and auranofin (Fig. 6, Table S6), achieving 100 and 86% regression in SIVs basket length, and 77 and 65% regression in ISVs length, respectively ($P < 0.001$, ANOVA). Importantly, treatments with this dose of gold(III) complexes did not caused any developmental defects, neither affected embryos survival, while auranofin and sunitinib at 1.25 μM showed serious toxic effects in zebrafish embryos, particularly on cardial function (large pericardial edema and markedly reduced heartbeat; $P < 0.001$, ANOVA) what progressively decreased embryos' survival up to 114 hpf (Figs. 6A and S7). Sunitinib is a clinically relevant metastatic drug, with pronounced cardiotoxicity being the major obstacle for its long-term application [67], which has also been demonstrated in this study.

We firstly assessed the anti-angiogenic activity of the gold(III) complexes and the corresponding ligands by determining IC_{50} values (the concentration upon which 50% of embryos displayed anti-angiogenic phenotype) and EC_{50} values for SIVs and ISVs (the effective concentration resulting in 50% decrease of SIVs or ISVs length compared to the vehicle solvent-treated control group). According to all three determined parameters (Table 2), tested compounds were ranked by their anti-angiogenic potential: sunitinib ≥ auranofin > **1** > **2** > 1,7-phen > 4,7-phen > $K[AuCl_4]$. It can be seen that complex **1** showed the strongest *in vivo* anti-angiogenic activity in the zebrafish model among the presently investigated gold(III)-phenanthroline complexes and the corresponding ligands. Again, improved anti-angiogenic properties of complexes in comparison to the ligands can be ascribed to the presence of the gold(III) centre.

Table 2

Toxicological parameters derived from the concentration-response curves for the assessment of toxicity and anti-angiogenic potential of gold(III) complexes **1** and **2**, 1,7- and 4,7-phenanthroline, $K[AuCl_4]$ and clinically used drugs auranofin and sunitinib.

	LC_{50}	EC_{50}	TI	IC_{50}	TW	EC_{50}	
						ISVs	SIVs
1,7-phen	43.05	22.98	1.87	9.10	4.7	21.06	14.13
$[AuCl_3$(1,7-phen-κ*N*7)$]$ (1)	127.74	50.72	2.52	2.89	44.2	5.62	2.09
4,7-phen	37.11	27.07	1.37	12.05	3.1	30.02	16.64
$[AuCl_3$(4,7-phen-κ*N*4)$]$ (2)	48.44	39.71	1.22	4.98	9.7	8.09	4.39
$K[AuCl_4]$	46.97	16.21	2.90	18.62	< 2.5	> 20	> 20
Auranofin	3.67	0.40	8.31	0.56	6.6	1.92	1.08
Sunitinib	1.08	0.72	1.50	0.50	2.16	1.76	1.06

LC_{50} – the concentration inducing the lethal effect of 50% embryos.
EC_{50} – the concentration affecting 50% embryos (survival and developmental defects).
IC_{50} values - the concentration upon which 50% of embryos displayed anti-angiogenic phenotype.
EC_{50} (SIVs and ISVs) - the effective concentration resulting in 50% decrease of SIVs basket or ISVs length compared to the DMF-treated control group.

In order to address whether the tested compounds have more specific effect towards inhibition of blood vessels formation in comparison to overall embryotoxicity (mortality), EC_{50} (the effective concentration resulting in toxic response at 50% of embryos) and the therapeutic window (TW; the ratio between LC_{50} and IC_{50} values) have been determined (Table 2). The obtained results clearly showed that both complexes have higher anti-angiogenic potential in comparison to both auranofin and sunitinib, particularly complex **1**. Moreover, determined IC_{50} values were far below respective EC_{50} values for **1** and **2**, but in case of auranofin and sunitinib very close or above the corresponding EC_{50}, respectively (Fig. S8). These findings indicate wide therapeutic window for gold(III)-phenanthroline complexes **1** and **2**, and an effective inhibition of angiogenesis at their subtoxic

concentrations, while an anti-angiogenic effect of auranofin and sunitinib would be achieved at the toxic concentrations range.

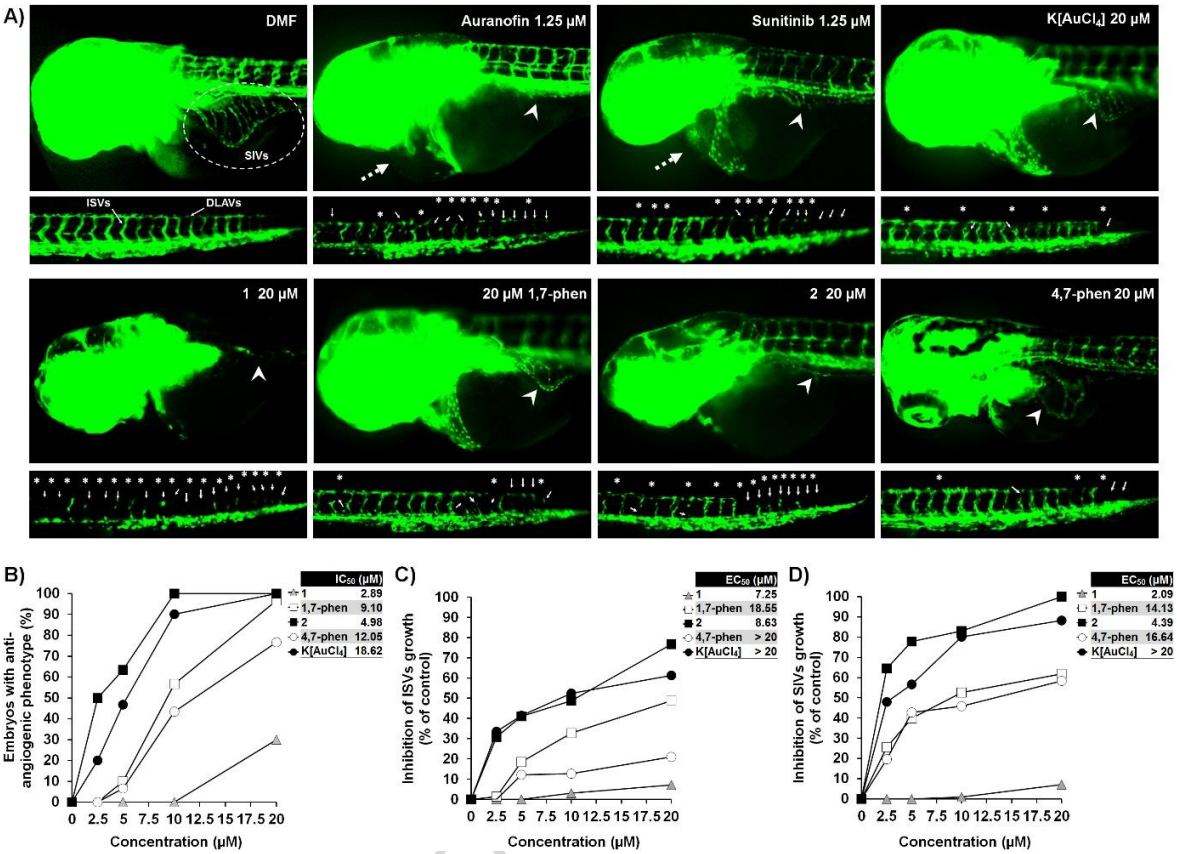

Fig. 6. *In vivo* effect of gold(III)-phenanthroline complexes on angiogenesis in zebrafish embryos in comparison to that of 1,7- and 4,7-phenanthroline, $K[AuCl_4]$ and clinically used drugs auranofin and sunitinib. (A) Effects on the treatments on subintestinal vessels (SIVs), intersegmental vessels (ISVs) and dorsal longitudinal anastomotic vessels (DLAVs) development in [*Tg*(*fli1*:EGFP)] zebrafish embryos assessed at 48 hpf (for ISVs and DLAVs) and 72 hpf (for SIVs). Normally developed SIVs, ISVs and DLAVs are designated in 0.035% DMF-treated embryo. Reduced SIVs (arrowhead), disrupted DLAVs (asterisk), thinner or reduced ISVs (arrow), and pericardial edema (dashed arrow) are denoted. (B) Anti-angiogenic response of zebrafish embryos upon different treatments. The quantification of the inhibition of ISVs angiogenesis (C) and SIVs basket angiogenesis (D).

Although numerous gold(I) and gold(III) complexes were reported for *in vitro* anti-proliferative potency, studies on their anti-angiogenic activity, solid tumor inhibition and toxicity in *in vivo* systems are rare [68-70]. The anti-angiogenic activity of auranofin, has only recently been discovered and described *in vivo* using [*Tg*(*fli1:EGFP*)] zebrafish embryos [49]. Prior to this, the inhibition of blood vessels development by gold(I) complexes with phosphine-naphthalimide and alkynyl(triphenylphosphine) has also been demonstrated in the zebrafish model [66,68]. These two gold(I) complexes influenced vessels development in 90% of the embryos only upon maximal non-lethal doses of 0.1 and 1 μM, respectively [66,69]. As mentioned earlier, gold(III)-phenanthroline complexes **1** and **2** were non-toxic even up to 20 μM, achieving comparable anti-angiogenic effect in zebrafish embryos to the mentioned gold(I) complexes upon the dose of 10 μM.

Contrary to gold(I) complexes, the diversity of reported gold(III) complexes with anti-angiogenic activity is far lower, involving 2-phenylpyridine gold(III) complexes with dithiocarbamate and gold(III) complexes with porphyrine, butilphenylpyridine and Schiff-base ligands [12-15]. Besides that, porphyrine-containing-gold(III) complex was shown to decrease intra-tumoral vascularization in melanoma-bearing mice [11]. Recently, we reported gold(III) complexes with L-histidine-containing dipeptides with anti-angiogenic potency in zebrafish model, achieving a comparable effect to 1.25 μM auranofin, but upon 30-fold higher concentrations [16]. Herein, we showed that gold(III)-phenanthroline complexes **1** and **2** have significantly higher anti-angiogenic activity and lower toxicity in comparison to the reported gold(III)-dipeptide complexes [16], confirming once again the crucial importance of the ligand nature for improvement of both efficacy and toxicity of anti-angiogenic compounds.

3.5. Molecular Docking Study

It is well documented that angiogenesis blockade can be achieved by single- or multi-targeting inhibition of major regulators of angiogenesis, such as the vascular endothelial growth factor receptors, the matrix metalloproteases and thioredoxin reductases. Among them, VEGFR-2 which drives endothelial cells survival, proliferation, and migration while increasing vascular permeability [71], MMP-2 and MMP-9 essential for the matrix remodeling around vessels and their sprouting, as well as cytosolic enzyme TrxR1, emerged as promising therapeutic strategies to combat angiogenesis-related diseases [71,72]. Although the exact molecular mechanisms responsible for anti-antiogenic activity of gold(III)-phenanthroline complexes and the corresponding ligands remain to be elucidated, recent study on the anti-angiogenic activity of 1,10-phenanthroline in zebrafish model system suggests that inhibition of matrix metalloproteases may be one of the possible mechanisms [20], although other mechanisms could not be ruled out. Therefore, we performed molecular docking study on VEGFR-2, MMP-2, MMP-9 and TrxR as *in silico* targets, with the aim to get insight into possible mechanisms of anti-angiogenic activity of gold(III)-phenanthroline complexes and the corresponding ligands. The results for the bonding mode of tested compounds and the binding energy for energetically most favorable binding modes are shown in Table 3 and Fig. 7. The best calculated pose for each of the studied compounds are presented in ESI, as well as two- and three-dimensional representation of their interactions with amino acids inside each target with identified hydrogen bonds and hydrophobic interactions (Figs. S9-16).

Table 3

The binding energy (in kcal/mol) for energetically most favorable binding sites of tested compounds in the selected targets as assessed by molecular docking.

Compound	Target			
	VEGFR-2	**MMP-2**	**MMP-9**	**TrxR1**
[$AuCl_3$(1,7-phen-κ*N7*)] (1)	-5.21	-3.99	-6.13	-4.77
1,7-phen	-3.94	-3.54	-4.29	-4.00
[$AuCl_3$(4,7-phen-κ*N4*)] (2)	-5.02	-3.67	-5.70	-4.71
4,7-phen	-4.01	-3.56	-4.27	-4.18
Auranofin	-1.79	-2.42	-1.76	-1.45
Sunitinib	-5.18	-3.62	-5.70	-6.34

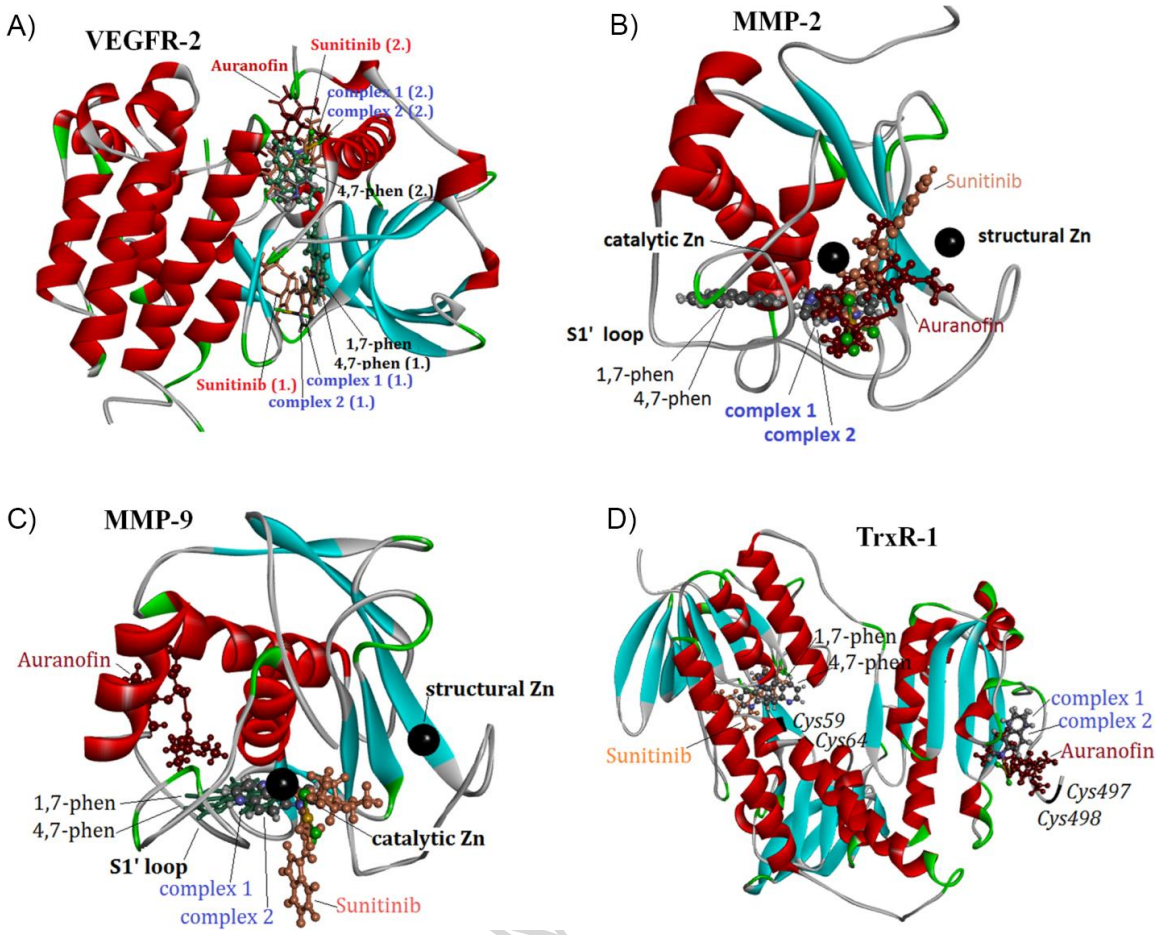

Fig. 7. The bonding sites of tested compounds inside the vascular endothelial growth factor receptor (VEGFR-2; A), matrix metalloprotease-2 (MMP-2; B), matrix metalloprotease-9 (MMP-9; C), and thioredoxin reductase (TrxR1; D). Tested compounds with the number of bonding sites higher than one are denoted with the number in brackets representing the order of the binding by affinity.

Docking simulation with VEGFR-2 showed that all investigated compounds had the tendency to bind in ATP-binding site of VEGFR-2 (the active site), differing in the number of molecules that can be bound, as well as in the values of binding energy (Fig. 7A and Table 3). The complexes **1** and **2** had significantly higher affinity for the active site (-5.21 and -5.02 kcal/mol, respectively) in comparison to 1,7- and 4,7-phen (-3.94 and -4.01 kcal/mol, respectively). This may be explained by the fact that phenanthroline ligands

formed weak hydrogen bonds and hydrophobic interactions with amino acids in the active site of VEGFR-2 (Fig. S13), while the complexes have additionally established electrostatic interactions with peptide carbonyl group by the Au(III) ion, what increased their binding affinity to the receptor. Interestingly, the binding affinities of **1** and **2** were comparable to those of sunitinib (-5.18 kcal/mol) (Fig. S13), for which is known to suppress angiogenesis by inhibition of VEGFRs, including VEGFR-2 [73]. Among tested compounds, the lowest affinity for the receptor VEGFR-2 was shown by auranofin (-1.79 kcal/mol), what may be attributed to its bulkiness and non-polar nature that sterically hindered its approach to the receptor's active center.

Result of docking study on MMP-2 and MMP-9 revealed the similar pattern of binding of each of tested compounds on both matrix metalloproteases, except of auranofin. While the complexes **1** and **2**, and sunitinib were bound to the active site of both enzymes, ligands 1,7- and 4,7-phen were bound to S1' pocket of these enzymes (Figs. 7C, S10, S11, S14 and S15). Such binding mode may be owing to a great sequence homology between MMP-2 and MMP-9, particularly in the catalytic site (Fig. 7B, C) [74]. Docking computation showed that complexes **1** and **2** in comparison to 1,7- and 4,7-phen had markedly higher binding affinity for MMP-9 (-6.13 and -5.70 kcal/mol, respectively, *vs.* -4.29 and -4.27 kcal/mol, respectively), and slightly higher for MMP-2 (-3.99 and -3.67 kcal/mol, respectively, *vs.* -3.54 and -3.56 kcal/mol, respectively). While ligands formed weak hydrogen bonds with non-polar amino acid residues from S1′ pocket of both MMPs, the coordination of phenanthrolines to Au(III) ion has led to increase of the compound surface, and therefore to increase of the number of amino acid residues with which each gold(III) complex **1** and **2** interacted. Additionally, the stacking and electrostatic interactions were established between Zn(II) ion of the catalytic centrum of enzymes and chlorido ligand in metal complexes (Fig. S14), what resulted in stronger binding of the complexes than

ligands to these enzymes. It is noteworthy that complexes had comparable or higher affinity for binding for both matrix metalloproteases than sunitinib, as in the case of VEGFR-2 (Table 3). On the other side, the lowest affinity for both MMPs has been shown by auranofin, what may be explained by its non-polar nature and steric hindrance for its binding to enzymes (Figs. S14 and S15).

Additionally, results of docking study showed that all tested compounds had greater binding affinity to MMP-9 than to MMP-2, except of auranofin which had higher affinity to MMP-2 (Table 3). It was previously shown that the conformational mobility of both active site and pockets of the matrix metalloproteases affected the inhibitory potency and selectivity of compounds [75]. Therefore, the conformational distortion of amino acid residues that occurs in the catalytic site of MMPs may explain the possible reason for higher affinity of tested compounds to MMP-9 than to MMP-2. However, the major difference between the catalytic domains of these matrix metalloproteases lies in the S1' pocket. While S1' pocket of MMP-2 is large hydrophobic channel and more deeper than S1' pocket of MMP-9, whereas the S1′ loop of MMP-2 is flexible to accommodate to more bulky ligands such as auranofin [74], S1′ pocket of MMP-9 is not sufficiently deep leaving auranofin bound outside the catalytic site of MMP-9 (Fig. 7C). Our results of docking computations for auranofin and sunitinib are in the agreement with the literature data which showed that auranofin attenuated MMP-2 activity, but leaving MMP-9 unaffected [76], while sunitinib decreased the activity of both MMP-2 and MMP-9 [77].

We found that each of gold(III)-phenanthroline complexes, as well as the corresponding ligands, was capable to bind to TrxR1 (Fig. 7D and S12), what is in the line with the docking results from our recent study demonstrating the interaction of gold(III)-peptide complexes with TrxR1 [16], and an extensive literature data confirming that gold(I) and gold(III) complexes are very effective TrxR inhibitors [78,79]. Complexes **1** and **2** (-4.77

and -4.7 kcal/mol, respectively) were bound stronger to TrxR1 compared to 1,7- and 4,7-phen (-4.00 and -4.18 kcal/mol, respectively), and markedly stronger than auranofin (-1.45 kcal/mol), what is similarly to pattern observed for VEGFR-2, MMP-2 and MMP-9 (Table 3). On, the other side, sunitinib (-6.34 kcal/mol) had the highest binding energy for TrxR1. Docking computation has also shown that complexes **1** and **2**, and auranofin had the affinity to selenocysteine residue located on C-terminal (Cys498, Cys499), while 1,7-, 4,7-phen and sunitinib had affinity to cysteine residues at the redox active site (Cys59, Cys64) at N-terminal domen (Figs. 7D and S16). The observed binding mode of **1**, **2** and auranofin to TrxR1 is in a line with the previous study demonstrating the interaction of gold-based inhibitors with accessible selenocysteine residue at C-terminal domen [80]. Higher affinity of gold(III)-phenanthroline complexes to selenocysteine in comparison to auranofin may be explained as in previous protein/ligand systems (VEGFR-2, MMP-2 and MMP-9). As selenocysteine is essentially involved in the catalytic cycle of TrxR1, and presents an attractive binding site to inhibitors [81], it is assumed that gold(III)-phenanthroline complexes could be inhibitors of TrxR1 enzyme. On the other site, the binding of 1,7-, 4,7-phen and sunitinib to the cysteine residues at the active site of TrxR1 is not probably accompanied by modifications of cysteine groups, what is otherwise necessary for the inhibition of TrxR1 activity, therefore these compounds should not be expected to act as inhibitors of TrxR1. As the support to our assumption is the finding of Zheng and coworkers, who demonstrated that sunitinib did not inhibit activity of TrxR1 in cancer cells [82].

4. Conclusions

Gold(III) complexes with 1,7- and 4,7-phenanthroline ligands, [$AuCl_3$(1,7-phen-κ*N*7)] (**1**) and [$AuCl_3$(4,7-phen-κ*N*4)] (**2**), were synthesized, spectroscopically and

crystallographically characterized and biologically evaluated for *in vitro* cytotoxic and *in vivo* embryotoxic and anti-angiogenic potential. The mode of coordination of these ligands towards the Au(III) ion was found to be governed by both steric and electronic factors. Gold(III) complexes along with the corresponding phenanthroline ligands show no significant anticancer activity and selectivity in terms of cancer *vs.* normal cell lines; nevertheless, they exert low cytotoxicity against normal cell line. Besides that, *in vivo* assessment performed on zebrafish embryos revealed that both complexes **1** and **2** were significantly less toxic than auranofin and sunitinib with the known anti-angiogenic potential, showing neither developmental nor cardiovascular toxicity. Moreover, the overall anti-angiogenic potential of gold(III)-phenanthroline complexes was markedly higher than that of auranofin and sunitinib drugs, making them good anti-angiogenic drug candidates. Molecular docking computations indicated that complexes **1** and **2** could suppress the angiogenesis by affecting the multiple targets involved in this process. The obtained results are encouraging in the light of the synthesis of the novel anti-angiogenic compounds, since the development of anti-angiogenic drugs targeting multiple sites presents the major challenge in the current anti-angiogenic therapy.

Appendix A. Supplementary data

Supplementary Material associated with this article includes Figs. S1-S16 and Tables S1-S6. Crystallographic data for **1** and **2** have been deposited with the Cambridge Crystallographic Data Centre (CCDC 1539103-1539104). Copies may be obtained free of charge on application to the Director, CCDC, 12 Union Road, Cambridge CB2 1EZ, UK (e-mail: deposit@chemcrys.cam.ac.uk).

Acknowledgements

This research was financially supported by the Ministry of Education, Science and Technological Development of Serbia (Grant No. 172036, 173048 and 174033) and the SupraMedChem@Balkans.Net SCOPES Institutional Partnership (Project No. IZ74Z0_160515). Dr. Ana Cvejic (Welcome Trust Sanger Institute, Cambridge, UK) is greatly acknowledged for providing transgenic zebrafish embryos. Dr. Milos Petkovic (Faculty of Pharmacy, University of Belgrade, Belgrade, Serbia) is greatly acknowledged for recording NMR spectra.

References

[1] M.E. Maragoudakis, Angiogenesis in health and disease, Gen. Pharmacol. 35 (2000) 225-226.

[2] J. Folkman, Angiogenesis in cancer, vascular, rheumatoid and other disease, Nat. Med. 1 (1995) 27-30.

[3] N. Ferrara, R.S. Kerbel, Angiogenesis as a therapeutic target, Nature 438 (2005) 967-974.

[4] M. Cesca, F. Bizzaro, M. Zucchetti, R. Giavazzi, Tumor delivery of chemotherapy combined with inhibitors of angiogenesis and vascular targeting agents, Front. Oncol. 3 (2013) 259.

[5] H. Büning, U.T. Hacker, Inhibitors of angiogenesis, in: T. Böldicke (Ed.), Protein Targeting Compounds: Prediction, Selection and Activity of Specific Inhibitors, Springer International Publishing, Cham, 2016, pp. 261-285.

[6] G. Bergers, D. Hanahan, Modes of resistance to anti-angiogenic therapy, Nat. Rev. Cancer 8 (2008) 592-603.

[7] K.D. Mjos, C. Orvig, Metallodrugs in medicinal inorganic chemistry, Chem. Rev. 114 (2014) 4540-4563.

[8] B. Bertrand, A. Casini, A golden future in medicinal inorganic chemistry: the promise of anticancer gold organometallic compounds, Dalton Trans. 43 (2014) 4209-4219.

[9] S. Nobili, E. Mini, I. Landini, C. Gabbiani, A. Casini, L. Messori, Gold compounds as anticancer agents: chemistry, cellular pharmacology, and preclinical studies, Med. Res. Rev. 30 (2010) 550-580.

[10] L. Ronconi, D. Fregona, The Midas touch in cancer chemotherapy: from platinum- to gold-dithiocarbamato complexes, Dalton Trans. (2009) 10670-10680.

[11] C.T. Lum, Z.F. Yang, H.Y. Li, R. W.-Y. Sun, S.T. Fan, R.T.P. Poon, M.C.M. Lin, C.-M. Che, H.F. Kung, Gold(III) compound is a novel chemocytotoxic agent for hepatocellular carcinoma, Int. J. Cancer 118 (2006) 1527-1538.

[12] R.W.-Y. Sun, C.K.-L. Li, D.-L. Ma, J.J. Yan, C.-N. Lok, C.-H. Leung, N. Zhu, C.-M. Che, Stable anticancer gold(III)–porphyrin complexes: effects of porphyrin structure, Chem. Eur. J. 16 (2010) 3097-3113.

[13] J.J. Yan, R.W.-Y. Sun, P. Wu, M.C.M. Lin, A.S.C. Chan, C.-M. Che, Encapsulation of dual cytotoxic and anti-angiogenic gold(III) complexes by gelatin-acacia microcapsules: *in vitro* and *in vivo* studies, Dalton Trans. 39 (2010) 7700-7705.

[14] J.-J. Zhang, K.-M. Ng, C.-N. Lok, R.W.-Y. Sun, C.-M. Che, Deubiquitinases as potential anti-cancer targets for gold(III) complexes, Chem. Commun. 49 (2013) 5153-5155.

[15] J.-J. Zhang, R.W.-Y. Sun, C.-M. Che, A dual cytotoxic and anti-angiogenic water-soluble gold(III) complex induces endoplasmic reticulum damage in HeLa cells, Chem. Commun. 48 (2012) 3388-3390.

[16] B. Warżajtis, B.Đ. Glišić, N.D. Savić, A. Pavic, S. Vojnovic, A. Veselinovic, J. Nikodinovic-Runic, U. Rychlewska, M.I. Djuran, Mononuclear gold(III) complexes with L-histidine-containing dipeptides: tuning the structural and biological properties by variation of the N-terminal amino acid and counter anion, Dalton Trans. 46 (2017) 2594-2608.

[17] J. Akhtar, A.A. Khan, Z. Ali, R. Haider, M. Shahar Yar, Structure-activity relationship (SAR) study and design strategies of nitrogen-containing heterocyclic moieties for their anticancer activities, Eur. J. Med. Chem. 125 (2017) 143-189.

[18] M. Asif, Some recent approaches of biologically active substituted pyridazine and phthalazine drugs, Curr. Med. Chem. 19 (2012) 2984-2991.

[19] D.J. Connolly, D. Cusack, T.P. O'Sullivan, P.J. Guiry, Synthesis of quinazolinones and quinazolines, Tetrahedron 61 (2005) 10153-10202.

[20] T. Ellis, B. Crawford, Experimental dissection of metalloproteinase inhibition-mediated and toxic effects of phenanthroline on zebrafish development, Int. J. Mol. Sci. 17 (2016) 1503.

[21] G. Accorsi, A. Listorti, K. Yoosaf, N. Armaroli, 1,10-Phenanthrolines: versatile building blocks for luminescent molecules, materials and metal complexes, Chem. Soc. Rev. 38 (2009) 1690-1700.

[22] M.A. Cinellu, L. Maiore, M. Manassero, A. Casini, M. Arca, H.-H. Fiebig, G. Kelter, E. Michelucci, G. Pieraccini, C. Gabbiani, L. Messori, $[Au_2(phen^{2Me})_2(\mu\text{-}O)_2](PF_6)_2$, a novel dinuclear gold(III) complex showing excellent antiproliferative properties, ACS Med. Chem. Lett. 1 (2010) 336-339.

[23] M. McCann, A. Kellett, K. Kavanagh, M. Devereux, A.L.S. Santos, Deciphering the antimicrobial activity of phenanthroline chelators, Curr. Med. Chem. 19 (2012) 2703-2714.

[24] M. McCann, A.L.S. Santos, B.A. da Silva, M.T.V. Romanos, A.S. Pyrrho, M. Devereux, K. Kavanagh, I. Fichtner, A. Kellett, *In vitro* and *in vivo* studies into the biological activities of 1,10-phenanthroline, 1,10-phenanthroline-5,6-dione and its copper(II) and silver(I) complexes, Toxicol. Res. 1 (2012) 47-54.

[25] W.D. McFadyen, L.P.G. Wakelin, I.A.G. Roos, V.A. Leopold, Activity of platinum(II) intercalating agents against murine leukemia L1210, J. Med. Chem. 28 (1985) 1113-1116.

[26] L. Messori, F. Abbate, G. Marcon, P. Orioli, M. Fontani, E. Mini, T. Mazzei, S. Carotti, T. O'Connell, P. Zanello, Gold(III) complexes as potential antitumor agents: solution chemistry and cytotoxic properties of some selected gold(III) compounds, J. Med. Chem. 43 (2000) 3541-3548.

[27] A. Prisecaru, V. McKee, O. Howe, G. Rochford, M. McCann, J. Colleran, M. Pour, N. Barron, N. Gathergood, A. Kellett, Regulating bioactivity of Cu^{2+} bis-1,10-phenanthroline artificial metallonucleases with sterically functionalized pendant carboxylates, J. Med. Chem. 56 (2013) 8599-8615.

[28] P.G. Sammes, G. Yahioglu, 1,10-Phenanthroline: a versatile ligand, Chem. Soc. Rev. 23 (1994) 327-334.

[29] Q.-Y. Zhu, J. Dai, Main group metal chalcogenidometalates with transition metal complexes of 1,10-phenanthroline and 2,2'-bipyridine, Coord. Chem. Rev. 330 (2017) 95-109.

[30] G.J. Lieschke, P.D. Currie, Animal models of human disease: zebrafish swim into view, Nat. Rev. Genet. 8 (2007) 353-367.

[31] T.P. Barros, W.K. Alderton, H.M. Reynolds, A.G. Roach, S. Berghmans, Zebrafish: an emerging technology for *in vivo* pharmacological assessment to identify potential safety liabilities in early drug discovery, Br. J. Pharmacol. 154 (2008) 1400-1413.

[32] C.A. MacRae, R.T. Peterson, Zebrafish as tools for drug discovery, Nat. Rev. Drug Discov. 14 (2015) 721-731.

[33] L.M. Cross, M.A. Cook, S. Lin, J.-N. Chen, A.L. Rubinstein, Rapid analysis of angiogenesis drugs in a live fluorescent zebrafish assay, Arterioscler. Thromb. Vasc. Biol. 23 (2003) 911-912.

[34] S. Rezzola, G. Paganini, F. Semeraro, M. Presta, C. Tobia, Zebrafish (*Danio rerio*) embryo as a platform for the identification of novel angiogenesis inhibitors of retinal vascular diseases, Biochim. Biophys. Acta Mol. Basis Dis. 1862 (2016) 1291-1296.

[35] T. Bartoš, S. Letzsch, M. Škarek, Z. Flegrová, P. Čupr, I. Holoubek, GFP assay as a sensitive eukaryotic screening model to detect toxic and genotoxic activity of azaarenes, Environ. Toxicol. 21 (2006) 343-348.

[36] B. Burýšková, K. Hilscherová, L. Bláha, B. Maršálek, I. Holoubek, Toxicity and modulations of biomarkers in *Xenopus laevis* embryos exposed to polycyclic aromatic hydrocarbons and their *N*-heterocyclic derivatives, Environ. Toxicol. 21 (2006) 590-598.

[37] B. Warżajtis, B.Đ. Glišić, N.S. Radulović, U. Rychlewska, M.I. Djuran, Gold(III) complexes with monodentate coordinated diazines: an evidence for strong electron-withdrawing effect of Au(III) ion, Polyhedron 79 (2014) 221-228.

[38] CrysAlis PRO, *Agilent Technologies*, Yarnton, Oxfordshire, England, 2014.

[39] G. Sheldrick, SHELXT - Integrated space-group and crystal-structure determination, Acta Crystallogr. Sect. A: Found. Crystallogr. 71 (2015) 3-8.

[40] G. Sheldrick, Crystal structure refinement with SHELXL, Acta Crystallogr. Sect. C: Struct. Chem. 71 (2015) 3-8.

[41] V. Barone, M. Cossi, Quantum calculation of molecular energies and energy gradients in solution by a conductor solvent model, J. Phys. Chem. A 102 (1998) 1995-2001.

[42] M.J. Frisch et al, Gaussian 09, revision D.01, Gaussian, Inc.: Wallingford CT, (2013).

[43] C. Morell, A. Grand, A. Toro-Labbé, New dual descriptor for chemical reactivity, J. Phys. Chem. A 109 (2005) 205-212.

[44] C. Morell, A. Grand, A. Toro-Labbé, Theoretical support for using the $\Delta f(r)$ descriptor, Chem. Phys. Lett. 425 (2006) 342-346.

[45] M.B. Hansen, S.E. Nielsen, K. Berg, Re-examination and further development of a precise and rapid dye method for measuring cell growth/cell kill, J. Immunol. Methods 119 (1989) 203-210.

[46] H. Lu, X. Li, J. Zhang, H. Shi, X. Zhu, X. He, Effects of cordycepin on HepG2 and EA.hy926 cells: potential antiproliferative, antimetastatic and anti-angiogenic effects on hepatocellular carcinoma, Oncol. Lett. 7 (2014) 15556-11562.

[47] OECD, OECD Guidelines for the Testing of Chemicals, Test no. 236, 2013.

[48] G. Chimote, J. Sreenivasan, N. Pawar, J. Subramanian, H. Sivaramakrishnan, S. Sharma, Comparison of effects of anti-angiogenic agents in the zebrafish efficacy – toxicity model for translational anti-angiogenic drug discovery, Drug Des. Devel. Ther. 8 (2014) 1107-1123.

[49] M.-F. He, X.-P. Gao, S.-C. Li, Z.-H. He, N. Chen, Y.-B. Wang, J.-X. She, Anti-angiogenic effect of auranofin on HUVECs *in vitro* and zebrafish *in vivo*, Eur. J. Pharmacol. 740 (2014) 240-247.

[50] G.M. Morris, R. Huey, W. Lindstrom, M.F. Sanner, R.K. Belew, D.S. Goodsell, A.J. Olson, AutoDock4 and AutoDockTools4: Automated docking with selective receptor flexibility, J. Comput. Chem. 30 (2009) 2785-2791.

[51] C.I. Bayly, P. Cieplak, W.D. Cornell, P.A. Kollman, A well-behaved electrostatic potential based method using charge restraints for deriving atomic charges: the RESP model, J. Phys. Chem. 97 (1993) 10269-10280.

[52] Dassault Systèmes BIOVIA, Discovery Studio Modeling Environment, Release 2017, 2016.

[53] T. Kromp, W.S. Sheldrick, C. Näther, Network motifs and thermal properties of copper(I) halide and pseudohalide coordination polymers with 1,7- and 4,7-phenanthroline, Z. Anorg. Allg. Chem. 629 (2003) 45-54.

[54] B.Đ. Glišić, M. Hoffmann, B. Warżajtis, M.S. Genčić, P.D. Blagojević, N.S. Radulović, U. Rychlewska, M.I. Djuran, Selectivity of the complexation reactions of four regioisomeric methylcamphorquinoxaline ligands with gold(III): X-ray, NMR and DFT investigations, Polyhedron 105 (2016) 137-149.

[55] B.Đ. Glišić, B. Warżajtis, N.S. Radulović, U. Rychlewska, M.I. Djuran, Gold(III) complexes with phenazine and quinoxaline: the role of molecular symmetry in intra- and intermolecular interactions, Polyhedron 87 (2015) 208-214.

[56] L. Cattalini, R.J.H. Clark, A. Orio, C.K. Poon, The infrared spectra (450 – 70 cm^{-1}) of square planar pyridine an substituted pyridine complexes of gold(III), Inorg. Chim. Acta 2 (1968) 62-64.

[57] B.Đ. Glišić, N.D. Savić, B. Warżajtis, L. Djokic, T. Ilic-Tomic, M. Antić, S. Radenković, J. Nikodinovic-Runic, U. Rychlewska, M.I. Djuran, Synthesis, structural characterization and biological evaluation of dinuclear gold(III) complexes with aromatic nitrogen-containing ligands: antimicrobial activity in relation to the complex nuclearity, MedChemComm 7 (2016) 1356-1366.

[58] R.G.A.R. Maclagan, S. Gronert, M. Meot-Ner, Protonated polycyclic aromatic nitrogen heterocyclics: proton affinities, polarizabilities, and atomic and ring charges of 1–5-ring ions, J. Phys. Chem. A 119 (2015) 127-139.

[59] V. Gandin, A.P. Fernandes, M.P. Rigobello, B. Dani, F. Sorrentino, F. Tisato, M. Björnstedt, A. Bindoli, A. Sturaro, R. Rella, C. Marzano, Cancer cell death induced by phosphine gold(I) compounds targeting thioredoxin reductase, Biochem. Pharmacol. 79 (2010) 90-101.

[60] L. Thornton, V. Dixit, L.O.N. Assad, T.P. Ribeiro, D.D. Queiroz, A. Kellett, A. Casey, J. Colleran, M.D. Pereira, G. Rochford, M. McCann, D. O'Shea, R. Dempsey, S. McClean, A.F.-A. Kia, M. Walsh, B. Creaven, O. Howe, M. Devereux, Water-soluble and photo-stable silver(I) dicarboxylate complexes containing 1,10-phenanthroline ligands: antimicrobial and anticancer chemotherapeutic potential, DNA interactions and antioxidant activity, J. Inorg. Biochem. 159 (2016) 120-132.

[61] A. Albert, Selective Toxicity: the physico-chemical basis of therapy, Springer, Netherlands, Dordrecht, 1985.

[62] D.S. Sigman, R. Landgraf, D.M. Perrin, L. Pearson, Nucleic acid chemistry of the cuprous complexes of 1,10-phenanthroline and derivatives, Metal Ions Biol. Syst. 33 (1999) 485-513.

[63] N.D. Savić, D.R. Milivojevic, B.Đ. Glišić, T. Ilic-Tomic, J. Veselinovic, A. Pavic, B. Vasiljevic, J. Nikodinovic-Runic, M.I. Djuran, A comparative antimicrobial and toxicological study of gold(III) and silver(I) complexes with aromatic nitrogen-containing heterocycles: synergistic activity and improved selectivity index of Au(III)/Ag(I) complexes mixture, RSC Advances 6 (2016) 13193-13206.

[64] F. Dai, L. Gao, Y. Zhao, C. Wang, S. Xie, Farrerol inhibited angiogenesis through Akt/mTOR, Erk and Jak2/Stat3 signal pathway, Phytomedicine 23 (2016) 686-693.

[65] S. Lin, Y. Zhao, Z. Ji, J. Ear, C.H. Chang, H. Zhang, C. Low-Kam, K. Yamada, H. Meng, X. Wang, R. Liu, S. Pokhrel, L. Mädler, R. Damoiseaux, T. Xia, H.A. Godwin, S. Lin, A.E. Nel, Zebrafish high-throughput screening to study the impact of dissolvable metal oxide nanoparticles on the hatching enzyme, ZHE1, Small 9 (2013) 1776-1785.

[66] A. Meyer, C.P. Bagowski, M. Kokoschka, M. Stefanopoulou, H. Alborzinia, S. Can, D.H. Vlecken, W.S. Sheldrick, S. Wölfl, I. Ott, On the biological properties of alkynyl phosphine gold(I) complexes. Angew. Chem. Int. Ed. 51 (2012) 8895-8899.

[67] M.H. Chen, R. Kerkelä, T. Force, Mechanisms of cardiac dysfunction associated with tyrosine kinase inhibitor cancer therapeutics, Circulation 118 (2008) 84-95.

[68] C.P. Bagowski, Y. You, H. Scheffler, D.H. Vlecken, D.J. Schmitz, I. Ott, Naphthalimide gold(I) phosphine complexes as anticancer metallodrugs, Dalton Trans. (2009) 10799-10805.

[69] I. Ott, X. Qian, Y. Xu, D.H.W. Vlecken, I.J. Marques, D. Kubutat, J. Will, W.S. Sheldrick, P. Jesse, A. Prokop, C.P. Bagowski, A gold(I) phosphine complex containing a naphthalimide ligand functions as a TrxR inhibiting antiproliferative agent and angiogenesis inhibitor, J. Med. Chem. 52 (2009) 763-770.

[70] T. Zou, A binuclear gold(I) complex with mixed bridging diphosphine and bis(*N*-heterocyclic carbene) ligands shows favorable thiol reactivity and effectively inhibits tumor growth and angiogenesis *in vivo*, in: Anti-Cancer N-Heterocyclic Carbene Complexes of Gold(III), Gold(I) and Platinum(II): Thiol "Switch-on" Fluorescent Probes, Thioredoxin Reductase Inhibitors and Endoplasmic Reticulum Targeting Agents, Springer Singapore, Singapore, 2016, pp. 101-134.

[71] F. Musumeci, M. Radi, C. Brullo, S. Schenone, Vascular endothelial growth factor (VEGF) receptors: drugs and new inhibitors, J. Med. Chem. 55 (2012) 10797-10822.

[72] S.M. Weis, D.A. Cheresh, Tumor angiogenesis: molecular pathways and therapeutic targets, Nat. Med. 17 (2011) 1359-1370.

[73] R. Roskoski Jr, Sunitinib: a VEGF and PDGF receptor protein kinase and angiogenesis inhibitor, Biochem. Biophys. Res. Comm. 356 (2007) 323-328.

[74] E. Bourguet, K. Brazhnik, A. Sukhanova, G. Moroy, S. Brassart-Pasco, A.-P. Martin, I. Villena, G. Bellon, J. Sapi, I. Nabiev, Design, synthesis, and use of MMP-2 inhibitor-conjugated quantum dots in functional biochemical assays. Bioconjugate Chem. 27 (2016) 1067-1081.

[75] O. Nicolotti, T.F. Miscioscia, F. Leonetti, G. Muncipinto, A. Carotti, Screening of matrix metalloproteinases available from the protein data bank: insights into biological functions, domain organization, and zinc binding groups, J. Chem. Inf. Model. 47 (2007) 2439-2448.

[76] J. Hošek, J. Vančo, P. Štarha, L. Paráková, Z. Trávníček, Effect of 2-chloro-substitution of adenine moiety in mixed-ligand gold(I) triphenylphosphine complexes on anti-inflammatory activity: the discrepancy between the *in vivo* and *in vitro* models, PLoS One 8 (2013) e82441.

[77] S.J. Jin, L. Ma, Q. Xu, L.P. Ren, Y.C. Ma, Sunitinib treatment inhibited human breast cancer cell migration through regulation furin interaction with substrates, Int. J. Clin. Exp. Med. 9 (2016) 2542-2548.

[78] S.J. Berners-Price, A. Filipovska, Gold compounds as therapeutic agents for human diseases, Metallomics 3 (2011) 863-873.

[79] A. Bindoli, M.P. Rigobello, G. Scutari, C. Gabbiani, A. Casini, L. Messori, Thioredoxin reductase: a target for gold compounds acting as potential anticancer drugs, Coord. Chem. Rev. 253 (2009) 1692-1707.

[80] C. Gabbiani, G. Mastrobuoni, F. Sorrentino, B. Dani, M.P. Rigobello, A. Bindoli, M.A. Cinellu, G. Pieraccini, L. Messori, A. Casini, Thioredoxin reductase, an emerging target for anticancer metallodrugs. Enzyme inhibition by cytotoxic gold(III) compounds studied with combined mass spectrometry and biochemical assays, MedChemComm 2 (2011) 50-54.

[81] S. Urig, K. Becker, On the potential of thioredoxin reductase inhibitors for cancer therapy, Semin. Cancer Biol. 16 (2006) 452-465.

[82] X. Zheng, Y. Zhang, L. Zhang, W. Xu, W. Ma, R. Sun, H. Zeng, Synergistic inhibition of sunitinib and ethaselen against human colorectal cancer cells proliferation, Biomed. Pharmacother. 83 (2016) 212-220.

Table and Figure Captions

Table 1

Cytotoxic activity expressed as IC_{50} value (μM) for gold(III) complexes **1** and **2** in comparison to that for 1,7- and 4,7-phenanthroline, $K[AuCl_4]$ and clinically used drug auranofin, upon treatment for 48 h.

Table 2

Toxicological parameters derived from the concentration-response curves for the assessment of toxicity and anti-angiogenic potential of gold(III) complexes **1** and **2**, 1,7- and 4,7-phenanthroline, $K[AuCl_4]$ and clinically used drugs auranofin and sunitinib.

Table 3

The binding energy (in kcal/mol) for energetically most favorable binding sites of tested compounds in the selected targets as assessed by molecular docking.

Fig. 1. (A) Schematic drawing of 1,7- and 4,7-phenanthroline ligands. The numeration of carbon atoms is in agreement with IUPAC recommendations for fused ring systems. (B) Molecular structures of $[AuCl_3$(1,7-phen-κ*N*7)] (**1**) and $[AuCl_3$(4,7-phen-κ*N*4)] (**2**) complexes. Thermal ellipsoids are drawn at 50% probability level. H-atoms are represented in an arbitrary scale.

Fig. 2. Diversity of intermolecular interactions in the crystal structure of **1**. H-bonds: dashed lines; Au···Cl: open lines; Cl···Cl: dotted lines; face-to-face stacking: shaded areas.

Fig. 3. (A) The structures of two possible mononuclear gold(III) complexes, $[AuCl_3$(1,7-phen-κ*N*7)] and $[AuCl_3$(1,7-phen-κ*N*1)], and their relative free energies calculated at the M06-2X(CPCM)/cc-pVTZ+LanL2TZ(f) level of theory. Dual descriptor isovalue surface (0.001 a.u.) for 1,7-phen: total (B), σ-orbital contribution (C) and π-orbital contribution (D). Nucleophilic and electrophilic regions are colored in red and blue, respectively.

Fig. 4. Wound healing migration of EA.hy926 cells. Effects of gold(III) complexes **1** and **2**, phenanthroline ligands and $K[AuCl_4]$, applied in concentration of 200 μM, on the migration of EA.hy926 cells after treatment for 6 h (B) in comparison to solvent (DMF) control at time 0 h (A). Auranofin (5 μM) was used as reference anti-angiogenic compound. For each treatment condition, eight measurements were taken randomly in each well. Data are presented as mean ± SD of two independent experiments with * $P < 0.05$; ** $P < 0.01$; *** $P < 0.001$ according to one-way ANOVA followed by the Bonferonni comparison test (C).

Fig. 5. Toxicity assay on zebrafish embryos exposed to gold(III) complexes **1** and **2**, ligands 1,7- and 4,7-phen, $K[AuCl_4]$ and auranofin expressed as LC_{50} values (μM). Morphology of zebrafish embryos at 114 hpf after treatment with 20 μM of **1**, **2**, ligands and $K[AuCl_4]$ (normal), and 1.25 μM of auranofin (teratogenic) are shown. Embryos upon auranofin treatment were retarded in the growth, had small or malformed head (bracket) and eyes (asterisk), large pericardial edema (arrow), non-resorbed egg yolk (NRY), signs of the tail lordosis (dashed arrow) and the necrotic tissue in the tail region (arrowhead).

Fig. 6. *In vivo* effect of gold(III)-phenanthroline complexes on angiogenesis in zebrafish embryos in comparison to that of 1,7- and 4,7-phenanthroline, $K[AuCl_4]$ and clinically used drugs auranofin and sunitinib. (A) Effects on the treatments on subintestinal vessels (SIVs), intersegmental vessels (ISVs) and dorsal longitudinal anastomotic vessels (DLAVs) development in [*Tg*(*fli1*:EGFP)] zebrafish embryos assessed at 48 hpf (for ISVs and DLAVs) and 72 hpf (for SIVs). Normally developed SIVs, ISVs and DLAVs are designated in 0.035% DMF-treated embryo. Reduced SIVs (arrowhead), disrupted DLAVs (asterisk), thinner or reduced ISVs (arrow), and pericardial edema (dashed arrow) are denoted. (B) Anti-angiogenic response of zebrafish embryos upon different treatments. The

quantification of the inhibition of ISVs angiogenesis (C) and SIVs basket angiogenesis (D).

Fig. 7. The bonding sites of tested compounds inside the vascular endothelial growth factor receptor (VEGFR-2; A), matrix metalloprotease-2 (MMP-2; B), matrix metalloprotease-9 (MMP-9; C), and thioredoxin reductase (TrxR1; D). Tested compounds with the number of bonding sites higher than one are denoted with the number in brackets representing the order of the binding by affinity.

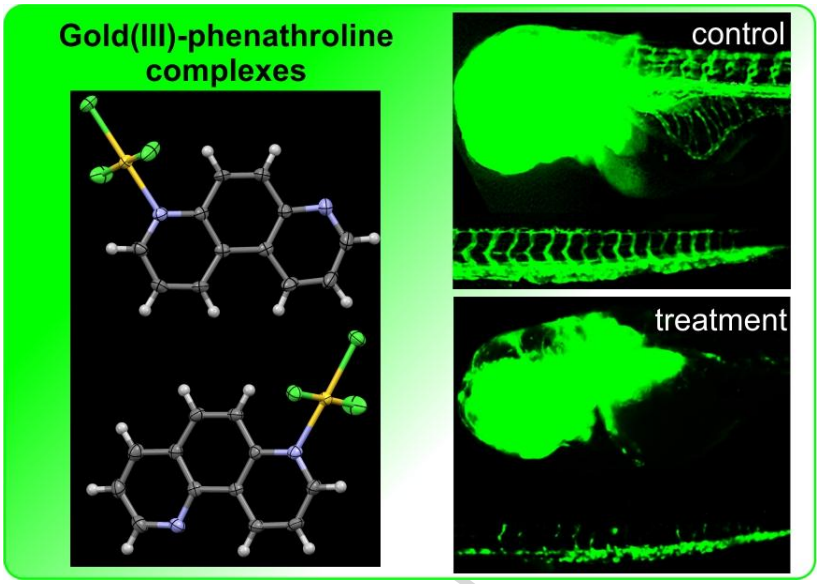

Graphical abstract

The anti-angiogenic potential of mononuclear gold(III) complexes with 1,7- and 4,7-phenanthroline ligands is markedly higher than that of the clinically relevant auranofin and sunitinib, making them good candidates for further development towards anti-angiogenic drugs.

Research Highlights

- Novel gold(III)-phenanthroline complexes were synthesized and characterized.
- Complexes and phenanthrolines have *in vitro* and *in vivo* anti-angiogenic activity.
- Complexes inhibit angiogenesis more effectively than auranofin and sunitinib.
- Complexes are less toxic both *in vitro* and *in vivo* than auranofin and sunitinib.
- Complexes could target the multiple major regulators of angiogenesis.